

Review

Recent Advances in Copper-Based Materials for Sustainable Environmental Applications

Sumalatha Bonthula ¹, Srinivasa Rao Bonthula ², Ramyakrishna Pothu ³ , Rajesh K. Srivastava ⁴,
Rajender Boddula ^{1,*} , Ahmed Bahgat Radwan ¹  and Noora Al-Qahtani ^{1,5,*} 

¹ Center for Advanced Materials (CAM), Qatar University, Doha 2713, Qatar; sumalatha.bonthula@gmail.com (S.B.); ahmedbahgat@qu.edu.qa (A.B.R.)

² Department of Physics, GITAM School of Science, GITAM (Deemed to be University), Visakhapatnam 530045, India; sbonthul@gitam.edu

³ School of Physics and Electronics, College of Chemistry and Chemical Engineering, Hunan University, Changsha 410082, China; research.ramyakrishna@gmail.com

⁴ Department of Biotechnology, GITAM School of Science, GITAM (Deemed to be University), Visakhapatnam 530045, India; sarosester@gmail.com

⁵ Central Laboratories Unit (CLU), Qatar University, Doha 2713, Qatar

* Correspondence: research.raaj@gmail.com (R.B.); noora.alqahtani@qu.edu.qa (N.A.-Q.)

Abstract: In recent years, copper-based nanomaterials have gained significant attention for their practical applications due to their cost-effectiveness, thermal stability, selectivity, high activity, and wide availability. This review focuses on the synthesis and extensive applications of copper nanomaterials in environmental catalysis, addressing knowledge gaps in pollution management. It highlights recent advancements in using copper-based nanomaterials for the remediation of heavy metals, organic pollutants, pharmaceuticals, and other contaminants. Also, it will be helpful to young researchers in improving the suitability of implementing copper-based nanomaterials correctly to establish and achieve sustainable goals for environmental remediation.

Keywords: copper nanomaterials; organic pollutants; sensors; antimicrobial; photocatalysts; CO₂ reduction; environmental remediation



Citation: Bonthula, S.; Bonthula, S.R.; Pothu, R.; Srivastava, R.K.; Boddula, R.; Radwan, A.B.; Al-Qahtani, N. Recent Advances in Copper-Based Materials for Sustainable Environmental Applications. *Sustain. Chem.* **2023**, *4*, 246–271. <https://doi.org/10.3390/suschem4030019>

Academic Editor: Raffaele Cucciniello

Received: 21 May 2023
Revised: 29 June 2023
Accepted: 10 July 2023
Published: 15 July 2023



Copyright: © 2023 by the authors. Licensee MDPI, Basel, Switzerland. This article is an open access article distributed under the terms and conditions of the Creative Commons Attribution (CC BY) license (<https://creativecommons.org/licenses/by/4.0/>).

1. Introduction

The economical and feasible design of nanomaterial catalysts for cutting-edge applications, as well as environmentally friendly catalytic processes and sustainable methods for developing synthetic strategies for catalysts, have received much attention from researchers in recent years. In this respect, scientific research is continually enhancing and enabling the synthesis of novel materials and applications [1]. Noble metal nanoparticles have a high degree of functionality due to their unique physical–chemical properties [2]. Their high stability, surface functionalization, and easy chemical synthesis makes the noble metallic nanoparticles, such as PtNPs, AuNPs, and AgNPs, extensively utilizable [3]. However, some earth-abundant and inexpensive metals have attracted attention in this regard over the expensive noble-metal catalysts that are used widely in conventional commercial chemical processes.

Owing to their high natural abundance, low cost, and numerous and practical simple syntheses, copper-based nanomaterials and nanocomposites are particularly appealing for research [4]. Due to their unique properties, copper nanoparticles are progressively becoming a key component in a variety of industries, such as energy, pharmaceutical, electronics, machinery, construction, engineering, environment, etc. In recent years, researchers focusing on sustainable approaches for environmentally friendly catalytic processes for various advanced applications. This review paper does not promote various chemical methods for synthesis; however, it aims to assist future research for an overall idea about

the various syntheses and applications of copper and copper-based nanomaterials in a sustainable way.

This section highlights key studies showcasing the potential of copper-based nanomaterials in environmental remediation. The novelty lies in Dennis et al.'s [5] review of the use of nanomaterials and plant extracts for wastewater micropollutant removal, assessing their efficacy, cost-effectiveness, and sustainability. Khalaj et al. investigate the toxicological and environmental effects of copper-based nanomaterials in treating persistent effluents, such as dyes, and their effects on the nanomaterial's reactivity [6]. Crisan et al. demonstrate the potential of copper nanoparticles as an alternative to antibiotics in the fight against multi-resistant bacteria strains [7]. Sandoval et al. discuss the generation of copper-based particles in the pretreatment, milling, and post-treatment steps, as well as the characterization methods used to analyze the resulting particles [8]. Hong et al. explore the effects of bimetallic catalysts on the selectivity of carbon dioxide reduction, emphasizing copper's role [9]. Naz et al. provide an overview of copper nanoparticles' synthesis, biomedical applications, and toxicological assessments [10]. Therefore, this present review article explores the potential of copper in various areas of environmental remediation such as the degradation of dyes, pharma products, wastewater treatment, and pesticides, and as a sensor for detecting various pollutants and reducing carbon dioxide (CO₂) emissions. This review explores the potential of copper-based nanomaterials, known for their abundance, cost-effectiveness, and practical synthesis methods, in various industries, and highlights the potential of copper in each application. For example, the use of copper in dye degradation has been shown to be effective in reducing water pollution, while copper can also be used in wastewater treatment to reduce levels of heavy metals. This review emphasizes the potential of copper-based nanomaterials in various environmental remediation applications and underlines the need for further research to fully harness its capabilities. The novelty of this work lies in presenting a sustainable perspective on the synthesis and applications of copper nanomaterials, stimulating further research in environmental remediation applications, and discussing potential challenges and future opportunities for the use of copper-based nanomaterials in environmental remediation.

2. Materials and Methodology

In comparison with other metals, copper is less toxic and inexpensive, and copper-based materials can be recycled and reused again [11]. Copper nanomaterial synthesis is simple, but proper experimental conditions with respect to time are somewhat challenging in comparison. Copper nanomaterial synthesis can be achieved by using green, chemical, and physical methods.

2.1. Synthesis of Cu Nanoparticles

This review is concentrated on various chemical methods involved recently in synthesis by varying different experimental conditions, and the materials can be further categorized into copper and copper-based nanoparticles as follows: (i) copper and copper oxide (CuO) nanoparticles, (ii) heterometal-doped copper nanomaterials, (iii) graphene oxide–copper nanomaterials, and (iv) copper-based metal–organic frameworks.

2.2. Synthesis of Copper and Copper Oxide Nanoparticles

There are two widely used approaches for synthesizing these nanomaterials: atomic-level precursors utilized to synthesize nano-sized materials, and bulk solids broken into smaller components. The second approach is widely used for its advantage in controlling the shape of the nanoparticles [12–15]. The synthesis of copper and the copper oxide nanoparticles are designed based on the final derivative, which centers or depends on four chemical reactions, namely oxidation, reduction, hydrolysis, and condensation. A diagram outlining the formation of CuO nanoflakes through nucleation growth, orientation attachment, and the Ostwald ripening process is presented in Figure 1.

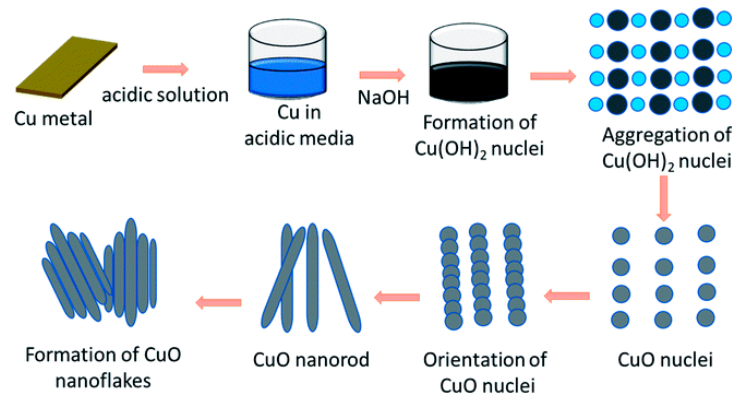


Figure 1. Illustration of the formation of the CuO nanoflakes. Adopted from Rumana Hossain et al. [16].

The following table outlines the various chemical synthesis procedures adopted for the synthesis of copper nanoparticles. Depending on the desired final nanomaterial, the synthesis can be proceed with different precursors, and the reaction environments and adopted synthetic methods (such as wet chemical, reverse micelle, microwave-assisted, etc.) can be changed, and are tabulated in Table 1.

Table 1. Reported experimental conditions for the **synthesis** of Cu and copper oxide NPs.

| Synthesized Nanomaterial | Method | Solvent | Precursor | Reducing Agent | Stabilizer/Binding Agent | Conditions | Product Description | Ref. |
|--------------------------|----------------------------|---------------------|---|---------------------|--------------------------|---|--------------------------------------|---------|
| CuO nanoflakes | Chemo-thermal | Water–acidic medium | Recovered Cu foil from FPCBs, Cu(OH) ₂ | NaOH | - | Decomposed at 520 °C | Width ~10 to 50 nm; length ~30–80 nm | [16] |
| Cu ₂ O | Reduction | Water | CuSO ₄ ·5H ₂ O, D-glucose, PVP, EG | NaOH | Ethylene glycol | Heated at 80 °C for 1 h, dried for 5 h in a vacuum oven at 55 °C | 150–200 nm | [17] |
| CuNPs | Aqueous solution reduction | Water | CuSO ₄ , H ₂ SO ₄ (pH = 3) | Ascorbic acid | PVP | 60 °C for 10 min. centrifuged, dried | - | [18] |
| Cu ₂ O | Aqueous solution reduction | Water | CuSO ₄ , NaOH (pH = 9–11) | Ascorbic acid | PVP | 60 °C for 4h. | - | [18] |
| CuNPs | Wet chemical | Octyl ether | Cu(acac) ₂ , EG, PVP, CuSO ₄ | 1,2-hexa decanediol | Oleic acid + Oleyl amine | 105 °C, 10 min; 150 to 200 °C, 30 min | 5–25 nm | [19] |
| Cu/Cu ₂ O | Chemical reduction | EG | ascorbic acid, acetone, NaOH | Ascorbic acid | PVP | 80 °C at 350 rpm for 36 h Dried at 6 h at 60 °C | 28/29 nm | [20] |
| CuO nanorods | Chemical precipitation | Water | SDS or SLS, Cu(NO ₃) ₂ | KOH, ammonia | - | Stirred at 700 rpm, centrifuged at 3 k rpm for 15 min, dried for 12 h at 60 °C, calcination 400 °C, 4 h | 20–40 nm | [21] |
| Cu NPs | Chemical reduction | EG | CuCl ₂ , PVP, NaOH | Ascorbic acid | - | 80 °C for 2h. | 34 nm | [22] |
| CuO NPs | Simple chemical reduction | Water | [Cu(OAc) ₂ (bpy)] | NaOH | - | 24 h at 160 °C | 15 nm | [23,24] |
| CuO NPs | hydrothermal reduction | Water | Cu(NO ₃) ₂ | NaOH | - | 6 h at 120 °C | 43 nm | [25] |
| CuS | Microwave hydrothermal | Water | Cu(OAc) ₂ ·H ₂ O, Thiourea | Thiourea | - | 6 min, 2 min on and 30 s off, repeat for 3 cycles. Filtered, dried at 60 °C for 6 h pH at 12.0, stirred continuously for 60 min at 60 °C, centrifuged at 13 k rpm at RT, dried at 70 °C for 5 h | 1.9 nm | [26] |
| Cu NPs | Agitation | Water | CuSO ₄ , PEI, NaOH | NaOH | PEI | 60 min at 60 °C, centrifuged at 13 k rpm at RT, dried at 70 °C for 5 h | 25 nm | [27] |

FPCBs—Flexible printed circuit boards; EG—Ethylene glycol; PVP—Polyvinyl pyrrolidone; SDS—Sodium dodecyl sulfate; SLS—Sodium lauryl sulphate; CTAB—Cetyltrimethyl ammonium bromide; PEI—Polyethylenimine.

2.3. Synthesis of Heterometal-Doped Copper-Based Nanocomposites

Various loadings of metal doping are carried out in nanomaterial synthesis to tailor the materials' cost, availability, and dispersibility; control the morphology; and adjust the materials' conductivity, mechanical, and magnetic properties, etc.

Khelifiac et al. [28] describe heterometals (Fe, Mn, Co, Zn, and Ni) doped to CuO which are designated as CuO:Fe, CuO:Mn, CuO:Co, CuO:Zn, and CuO:Ni, respectively, which are synthesized using copper sulfate as the primary precursor through a coprecipitation method.

CuO nanoparticles can be synthesized using a chemical reduction method with the aqueous solution of 1 M copper sulfate solution and sodium hydroxide, while maintaining the pH and temperature with constant stirring and other experimental conditions. A similar procedure is followed for doping of all the heterometals into CuO. The precipitate hence formed is annealed at 500 °C for 4 h to obtain a pure nanomaterial to enhance the crystalline quality of the synthesized powder. In another modified chemical reduction [29] method for the synthesis of Cu₂O nanoparticles, the dopant elements, such as La, Mg, and Mn are doped while using the 20 mM ethanolic solutions of lanthanum nitrate, magnesium nitrate, and manganese nitrate, respectively [30–32]. Ce-doped CuO is synthesized by using the microwave irradiation method to find microstructural changes from spherical to rod-like structures with optical band gap variation from 3.63 to 3.13 eV [33]. A study disclosed the synthesis of Zr doping on CuO via the Pechini method and enhanced antibacterial properties were investigated [34].

Similarly, many synthesis methods have been adopted to obtain doped Cu₂O nanostructures, such as electrodeposition [35], chemical displacement [36], hydrothermal synthesis [37], biosynthesis [38,39], chemical vapor deposition [40,41], pulsed laser deposition [42], solvothermal synthesis [43,44], and spray pyrolysis [40,45]. Table 2 reports the various experimental conditions for the synthesis of heterometal-doped copper nanomaterials.

Table 2. Reported experimental conditions for the synthesis of heterometal-doped copper NPs.

| Nanomaterial | Method | Solvent | Precursor | Reducing Agent/Stabilizer | Conditions | Product Description | Ref. |
|-------------------------|---------------------------------|-------------------------------------|---|---|--|---|------|
| h-BN (Ag/Cu) | Agitation followed by growing | Water | CuCl ₂ , h-BN, Trimethoxy silane | NH ₂ NH ₂ ·H ₂ O | 6 h stirring at room temperature, drying overnight at 60 °C | - | [46] |
| CuNPs /DA | Co-pre capitiation | Ethanol | CuSO ₄ ·5H ₂ O, 1% chitosan | NaOH, ascorbic acid | Stirring followed by irradiation at 20 kGy linear accelerator and drying at 80 °C | 20 nm | [47] |
| SnO ₂ /CuNPs | Co-precipitation | Water | SnCl ₂ ·2H ₂ O, Cu(OAc) ₂ ·H ₂ O | Ammonia | pH maintained at 9.8 and heated at 50 °C for 2 h | 25–35 nm | [48] |
| Cu-TiO ₂ | Reverse micelle sol-gel | Water | Cu(NO ₃) ₂ ·3H ₂ O, Triton X-114, Toulene, Hexane | TTIP | Stirring for 15 h at 700 rpm. Centrifuging for 10 min at 8 krpm, 18 h 130 °C drying, calcination for 4 h at 400 °C | 5.79 nm ³ /0.0839 cm ³ /g | [49] |
| CeO ₂ -CuO | Flame spray pyrolysis (FSP) | 1:2 xylene and 2-ethylhexanoic acid | Cerium (II) ethyl hexanoate, Soligen copper 8 | - | FSP followed by annealing at 500 °C, 5 h | 13.6 nm | [50] |
| CuO-GdO | Hydrothermal | Water | GdCl ₃ , CuCl ₂ | NH ₄ OH | Autoclave 150 °C, 16 h; calcined at 500 °C | | [51] |
| CuS QDs@ ZnO | Microwave-assisted hydrothermal | Water | Zn(NO ₃) ₂ ·3H ₂ O, HMT, | Thiourea | Stirring for 6 min, irradiated and dried in oven at 70 °C for 10 h | 36.5 nm | [26] |
| Cu/CuO-ZnO | Solution combustion synthesis | Water | Cu(OAc) ₂ ·H ₂ O, Cu(NO ₃) ₂ ·3H ₂ O, Zn(NO ₃) ₂ ·3H ₂ O, PVA | Urea | Dehydrated by heating to 110 °C, powder obtained calcined at 500 °C for 3 h. | 15–50 nm | [52] |
| CuO@ AgO/ZnO | Hydrothermal synthesis | Water | Zn(OAc) ₂ , CuSO ₄ , AgNO ₃ | NaOH | Autoclave at 185 °C for 12 h, desiccated at 70 °C for 8 h, calcinated at 600 °C for 5 h | 85 nm | [53] |
| Ni/CuO | Hydrothermal synthesis | Water | CuSO ₄ , NiSO ₄ | NaOH | Hydrothermal 180 °C for 12 h, dried at 80 °C for 12 h | 19 to 28 nm | [54] |

h-BN—Hexagonal boron nitride; Diatomite (DA) with the main component of silica (SiO₂). TTIP—Titanium tetra iso propoxide; PVA—Polyvinyl alcohol; NH₂NH₂·H₂O—Hydrazine hydrate; HMT—hexamethylenetetraamine.

2.4. Synthesis of Graphene Oxide (GO)-Based Copper Nanocomposites

For the synthesis of efficient heterogeneous catalysts, graphene has been widely used as a stable and suitable substrate for Nanocatalysts [55,56]. During transformations, its high conductivity can accelerate the transfer of electrons [57]. As a result, metal nanocatalysts based on graphene may perhaps promote electrons to facilitate the reduction efficiency. In fact, when graphene is combined with less reactive Nanocatalysts, this can also produce highly active hybrid nanocomposite catalysts [58]. In an article, CuCl_2 and GO solutions were taken as precursors and synthesized by using a hydrothermal process through heating up to $150\text{ }^\circ\text{C}$ for 12 h to obtain a CuO-GO nanocomposite. The catalyst was effective in the successful reduction of nitroaromatics [59]. In another synthesis of rGO-Ag nanoparticles, AgNO_3 was used and an rGO solution was added to AgNO_3 and reduced while using NaBH_4 . For the rGO-Cu nanoparticle synthesis, AgNO_3 was replaced with $\text{Cu}(\text{OAc})_2$ [60].

In another modified synthesis [61] for a non-enzymatic biosensor to detect glucose, the GO-CuO-FTO nanocomposite was prepared. The initial synthesis was comprised of a nanobelt formation of GO-CuO with a hydrothermal reduction of GO and CuO. This was followed by preparing GO-CuO-FTO using a fluorine-doped tin oxide (FTO) substrate. The following Table 3 reports the recent procedures and the experimental conditions for the synthesis of GO-based copper nanomaterials.

Table 3. Reported experimental conditions for the synthesis of GO-based copper based materials.

| Nanomaterial | Method | Solvent | Precursor | Reducing Agent /Stabilizer | Conditions | Product Description | Application | Ref. |
|--------------------------------------|-------------------------------------|-------------------------------|--|--------------------------------------|---|---|--|------|
| GO/CuO | Simple chemical reduction | Water | CuO, graphite powder | NaOH | Stirring for half an hour to $100\text{ }^\circ\text{C}$ | 70–200 nm | Glucose | [61] |
| CuO/GO-DE | Ultrasonic impregnation method | Water | $\text{Cu}(\text{NO}_3)_2$ | NaOH | Ultrasonication 30 min with reducing agent, filtered, dried 110° for 2 h | 0.52699 (μm) (pore diameter) | Ciprofloxacin degradation | [62] |
| CuO-rGO | Simple liquid approach | Water | $\text{Cu}(\text{OAc})_2$ | Ammonia | Reflux 2 h, agitated 1 h. Centrifuged, dried for 10 h at $80\text{ }^\circ\text{C}$ | 21.68 nm | Ascorbic acid | [63] |
| CPA/N-SWCNTS-GO-CE/CuO nanocomposite | Chemical oxidative copolymerization | 0.5 M H_2SO_4 | CuO, Graphene, PPDA, TPA, Aniline | Ammonia | Ultrasonication for 30 min, stirring at $0\text{--}4\text{ }^\circ\text{C}$ in N_2 atm. 24 h, black powder dried at $60\text{ }^\circ\text{C}$ for 24 h. | - | Methyl orange degradation | [64] |
| CuO@GO | Reflux | Water/ isopropanol | $\text{Cu}(\text{OAc})_2$, graphite, NaNO_3 , | $\text{NH}_4\text{OH}/\text{KMnO}_4$ | Stirring at $82\text{ }^\circ\text{C}$ for 2 h, dried at $60\text{ }^\circ\text{C}$ in hot air oven overnight | - | Synthesis of alcohols to carbonyl compounds | [65] |
| CuO-GO-Ag | Chemical reduction | | CuSO_4 , GO nanosheets, SDSAg nanoparticles | Ammonia | The entire solution is sonicated for 1 h, pH set to 10.0, heated in oil bath, kept at $112\text{ }^\circ\text{C}$ for 30 min, dried in hot air for 10 h, annealed 4 h at $400\text{ }^\circ\text{C}$ | 5–10 μm | Antibacterial properties | [66] |
| CuO/IL-rGO | drop on SPCE | Water | Copper oxide, reduced graphene oxide, ionic liquid (IL) | - | drop on screen-printed carbon electrode (SPCE) | 70–200 nm | Glucose levels in human urine and electrolytes | [67] |
| CuO-Cu ₂ O/GO | Hydrothermal synthesis | Water | Copper acetate, CTAB | CTAB | Autoclaved $160\text{ }^\circ\text{C}$ for 12 h, dried at $60\text{ }^\circ\text{C}$ for 24 h | 0.21–0.24 nm | Organic dyes and tetracycline pollutants | [68] |
| rGO-ZnO/CuO | Microwave irradiation | Water | Graphite powder, Zinc acetate, copper nitrate, NaOH, PEG | NaOH /PEG | Stirring for 20 min at $70\text{ }^\circ\text{C}$ with the successive addition of each precursor at pH 10, MW 10 min, dried $80\text{ }^\circ\text{C}$ for 6 h and then $200\text{ }^\circ\text{C}$ for 2 h | Length 230–780 nm; diameter 30–96 nm | 4-nitrophenol, methylene blue | [69] |

Table 3. Cont.

| Nanomaterial | Method | Solvent | Precursor | Reducing Agent /Stabilizer | Conditions | Product Description | Application | Ref. |
|--|-----------------|---------|--|---|---|---------------------|------------------------------|------|
| Cu@Ni/rGO | Ultrasonication | Water | Graphite powder, NaNO ₃ , KMnO ₄ , NiCl ₂ ·6H ₂ O, CuSO ₄ | NaOH, NH ₂ NH ₂ ·H ₂ O | Ultrasonicated for 15 min, NH ₂ NH ₂ ·H ₂ O with NaBH ₄ added under N ₂ atm. for 30 min and filtered, washed and dried at RT | - | 4-nitrophenol hydrogenation | [70] |
| rGO/bimetallic Fe _x Cu _y | Reflux | Water | Fe(OAc) ₂ , Cu(OAc) ₂ , graphite oxide | NaBH ₄ , EG, NaOH | The contents were refluxed for 5 h at 85 °C, centrifuged, and frozen for later use | 34.7 to 44.5 nm | Cyclophosphamide degradation | [71] |

GO-DE—Graphene oxide–diatomaceous earth; PPDA—p-phenylenediamine; TPA—Triphenylamine; SDS—Sodium dodecyl sulphate; CTAB—Cetyltrimethylammonium bromide; PEG—Polyethylene glycol; MW—Microwave.

2.5. Synthesis of Copper-Based Organic and Metal–Organic Frameworks

A copper metal–organic framework (Cu-MOF) was synthesized via the solvothermal method from Cu(NO₃)₂·3H₂O and 1,3,5-benzenetricarboxylic acid ligand following the mixture of solvents (DMF, C₂H₅OH, and H₂O). The experimental procedure was regular; however, the homogenous mixture was kept aside for 3 days to obtain the precipitate [72]. In the preparation of CuO nanoparticles/Ti₃C₂T_x MXene, the solution containing CuO nanoparticles was placed in an ultrasonic bath and sonicated at room temperature for 20 min in order to disperse them. Afterwards, a designated amount (10, 20, 30, 40 wt %) of Ti₃C₂T_x MXene powder was added to the solution, followed by stirring at 500 rpm for 10 min. The mixture was then filtered, washed with ethanol, and dried at 70 °C for 12 h. The sample with 30 wt. % of Ti₃C₂T_x-MXene was chosen for further characterization [73].

An electrochemically activated copper nitroprusside (CuNPr)-based sensor for the ultra-trace detection of acetaldehyde (AcH) has also been developed. First, 0.1 M sodium nitroprusside was added dropwise to a copper chloride solution of equal concentration and stirred for 30 min at room temperature. Then, the formed greenish-blue colloid precipitate was washed and then dried at 50 °C. The oxidation of AcH to acetate ions by CuNPr was studied using in situ spectro-electrochemical analyses. The sensor CuNPr/GCE exhibited a limit of detection towards AcH as low as 41×10^{-8} M. The sensing was successfully employed on a red wine sample [74]. A study demonstrated the potential of a graphene-based composite through supramolecular assembly of graphene nanosheets, 4-hydroxyquinoline (4HQ), and copper (II) ions (4HQ-rGO/Cu) as a room-temperature acetic acid gas sensor in a practical application. When acetic acid was attached, the supramolecular assembly showed an enhanced sensing performance at room temperature due to the accelerated charge transfer between the graphene nanosheets and 4HQ molecules. The copper (II) ions also acted as the main active site for gas adsorption, and the as-fabricated sensor exhibited a high response time within 5 s at room temperature [75].

A research study focused on the magnetic adsorption material polyaniline (PANI) with an amino-functional group combined with CuFe₂O₄ (CuFe₂O₄/PANI nanocomposite). The coprecipitation technique was adopted for the preparation of CuFe₂O₄ nanoparticles. CuFe₂O₄/PANI nanocomposite was prepared by chemical in situ polymerization. The material showed an extremely high maximum adsorption capacity of 322.6 mg/g for the removal of uranyl ions from wastewater at a pH of 4. The adsorption process followed the quasi-second-order kinetic equation. It was also stated that the material has stable adsorption performance for uranyl ions after five cycles of recovery in acid medium [76].

The study presents a novel approach for the synthesis of Pd-Cu alloy nanoparticles encapsulated in carbon nanopillar arrays (Pd-Cu@HPCN) which are promising oxygen evolution electrocatalysts. Figure 2 shows that, by using Cu-based MOF materials as a

framework, the author disclosed a versatile technique to produce a Pd-Cu alloy enclosed within porous carbon nanopillar arrays.

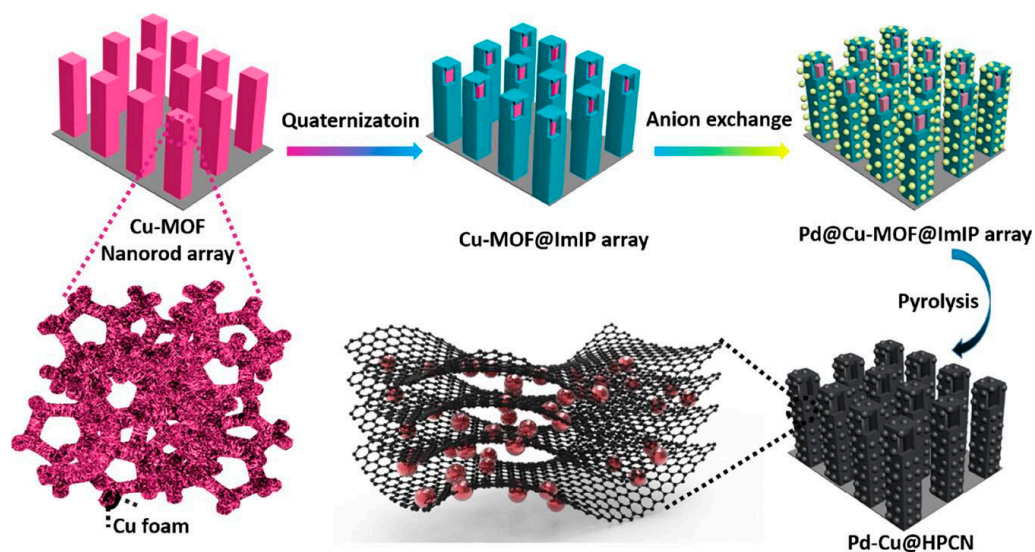


Figure 2. Scheme illustrating the fabrication of the hollow carbon nanopillar arrays encapsulated with Pd–Cu Alloy nanoparticles [77].

Figure 2 shows that the synthesis involves the preparation of a core–shell structured MOF@imidazolium-based ionic polymers (ImIPs) template and the subsequent decomposition of the inner Cu–MOFs when an anion exchange occurs between sodium tetrachloropalladate in solution and bromides in the external ImIP shell. The resulting Pd–Cu@HO-ImIP array is then topotactically transformed to generate Pd–Cu@HNPC [77].

3. Characterization Methods for Copper-Based Nanomaterials

Several techniques have been employed to analyze copper oxide and its composites. These include elemental composition analysis techniques such as ICP-MS, ICP-OES, SEM-EDS, and XAS. Structural characterization is performed using XRD and XPS, while morphological analysis relies on TEM and SEM. Surface area and pore size distribution are assessed through Brunauer–Emmett–Teller (BET) measurements, and optical properties are examined using instruments like UV-Vis spectrophotometers and UV-Vis-Near IR analyzers [32]. These techniques enable the measurement of various properties, such as size and shape, which are crucial for characterizing nanomaterials. These measurements serve as a basis for reproducing experiments. Figure 3 illustrates the characterization techniques employed for copper nanoparticles [78].

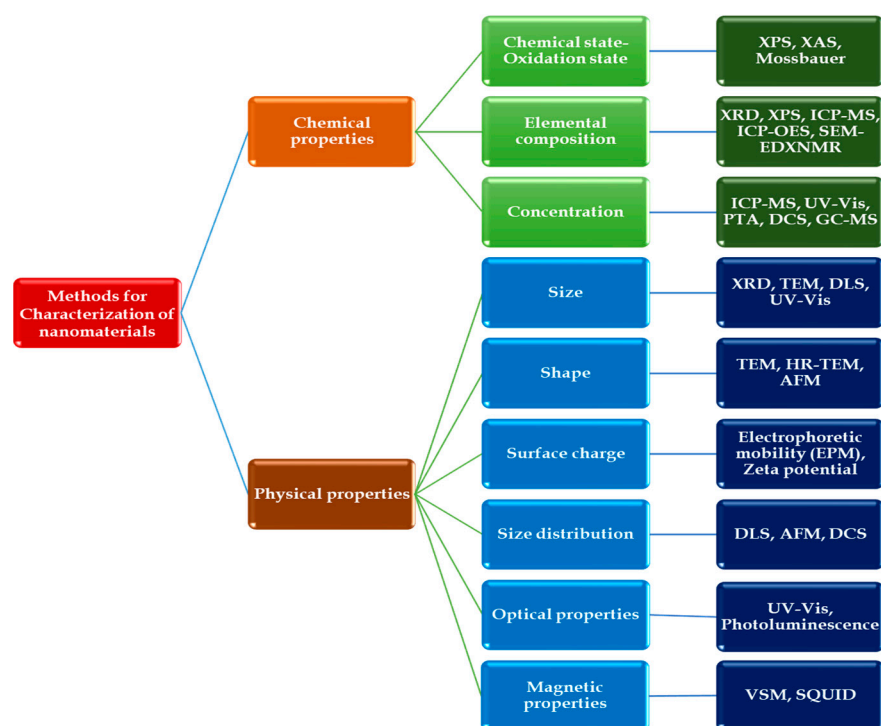


Figure 3. Various nanoparticle characterization techniques with respect to physical and chemical properties: Atomic force microscopy (AFM), Superconducting quantum interference device magnetometry (SQUID), Photoluminescence (PL), Dynamic light scattering (DLS), Differential centrifugal sedimentation (DCS), UV-Vis Spectroscopy (UV-Vis), X-ray Diffraction (XRD), X-ray Photoelectron Spectroscopy (XPS), X-ray Absorption Spectroscopy (XAS), Inductively Coupled Plasma–Mass Spectrometry (ICP-MS), Inductively Coupled Plasma Optical Emission Spectrometry (ICP-OES), Transmission electron microscopy (TEM), High-Resolution Transmission Electron Microscopy (HRTEM), Electrophoretic mobility (EPM), Vibrating sample magnetometry (VSM).

4. Copper-Based Nanomaterials for Environmental Pollution Management

4.1. Copper-Based Nanomaterials in Photodegradation of Industrial Dyes/Removal of Dyes

Recent advances in the food, paper, leather, and textile industries have rapidly increased the usage of organic dyes. This high usage of dyes, which are the main sources of organic pollution in various industries, has led to a global concern [79–81]. Since these dyes are extremely persistent, and carcinogenic to humans and other living things, even very low quantities of chemical pollutants in wastewater cannot be eliminated easily by regular methods such as sedimentation and ordinary chemical degradation [79,82]. Hence, removal of these effluents is important. Therefore, a sustainable technique for the removal of such effluents is essential to remove these hazardous pollutants, and therefore efficient catalytic reduction and photocatalytic degradation are essential [83–85]. The two oxidation states of copper, Cu^{2+} and Cu^+ , act as electron trappers, leading to a higher degradation efficiency of copper nanoparticles. The catalytic property of CuNPs was observed in the reduction activity of Xanthene dye that could be applicable in biological sensing [86]. In a study, to treat textile wastewater, it was observed that the degradation activity of CuO NPs was higher than $\text{Ni@Fe}_3\text{O}_4$ against organic dyes such as Congo red, methylene blue, and Rhodamine B [87], and also showed reduction of 4-nitrophenol [88].

Hamed et al. [89] concluded that copper nanoparticles decorated with alginate/cobalt-doped cerium oxide composite beads are a promising photocatalyst for the reduction and photodegradation of organic dyes. This composite material is effective at degrading a wide range of organic dyes, with no additional energy source required. Table 4 shows the comparison of the photocatalytic efficacy of the copper-based nanomaterials concerning various dye pollutants.

Table 4. Table showing the photocatalytic efficacy of copper-based nanomaterials for various dyes.

| SI.No | Copper-Based Nanoparticles | Synthesis Method | Pollutant | Degradation Time (min.) | Rate Constant (min^{-1}) Degradation Efficiency | Ref. | |
|-------|----------------------------|---|---------------------------------|-------------------------|---|----------------|------|
| 1 | Cu@Alg/Co-CeO ₂ | One-pot synthesis | ArO (0.07 mM) | 300 | 75.26% | [89] | |
| | | | CR (0.07 mM) | 270 | 33.65% | | |
| | | | MB (0.07 mM) | 180 | 49.70% | | |
| | | | MO (0.07mM) | 240 | 45.54% | | |
| 2 | Cu/GO/TiO ₂ | Quartz boat sealed in a furnace and argon gas flown | MB/Cu (1%)-TiO ₂ -GO | 141.1 | 4.91 min^{-1} | [90] | |
| | | | MB/Cu (2%)-TiO ₂ -GO | 112.7 | 6.15 min^{-1} | | |
| | | | MB/Cu (3%)-TiO ₂ -GO | 60.8 | 11.40 min^{-1} | | |
| 3 | NiO/CuO | Co-precipitation | RB-5 | 120 | 93% | [91] | |
| | | | RR-2 | | 92% | | |
| | | | O-II | | 96% | | |
| 4 | 2D Cu nanosheets | Oriented attachment mechanism | MB | 20 | 95% | [92] | |
| 5 | CuO | Thermal decomposition | RhB | 150 | 93% | [93] | |
| 6 | Porous CuO nanosheets | Precipitation | AR | 6 | 96.99% | [94] | |
| | | | | | | | |
| 7 | Copper sulfide | Precipitation | CV | 120 | CuS1 | 56.9% (0.0066) | [95] |
| | | | | | CuS2 | 72.8% (0.0104) | |
| | | | | | CuS3 | 84.6% (0.0145) | |
| | | | MB | | CuS1 | 31.8% (0.006) | |
| | | | | | CuS2 | 60.1% (0.0078) | |
| | | | | | CuS3 | 99.2% (0.0481) | |
| | | | | | CuS1 | 26.5% (0.0025) | |
| RhB | CuS2 | 53% (0.0062) | | | | | |
| | CuS3 | 81.4% (0.0127) | | | | | |
| 8 | Cu ₂ O | Simple chemical reduction | Congo red | 180 | 90% | [96] | |
| 9 | CuO | Simple chemical reduction | MB | 60 | 55.5% | [97] | |

Allura red (AR), Methyl orange (MO), Reactive red (RR), Orange-II (O-II), Acridine orange (ArO), Congo red (CR), Rhodamine B (RhB), Reactive black (RB), Crystal Violet (CV), Methylene blue (MB).

4.2. Copper in Reduction of Other Heavy Metal Contamination

In developing countries, the industrial sector is rapidly increasing, and the heavy harmful metals from these industries, such as metal and mining, batteries, paper, pesticides, chemical and petrochemical, textile, leather, cement, etc., are released into water bodies. These toxic heavy metals, such as lead (Pb), chromium (Cr), cadmium (Cd), arsenic (As), etc., do not break down further in the environment and accumulate into the vital organs of animals, causing various chronic diseases and death in extreme cases [98–102].

A highly porous material, Cu-DPA MOF [103], was synthesized for the removal of heavy metals from wastewater. The adsorption parameters, such as pH value, contact time, initial metals concentration, and Cu-MOF dosage, exhibited significant adsorption processes in the removal of heavy metals such as Pb, Cd, and Cr. The effect of adsorbent dose, pH, metal ion concentration, contact time, and time of mixing to reach equilibrium for these heavy metals by Cu-DPA MOF was determined through batch adsorption experiments. An optimized procedure was performed in order to carry out this procedure on wastewater containing Cd, Cr, and Pb [103]. An overview of some of the copper nanomaterials associated with the removal of heavy metal ions is tabulated in Table 5. The adsorption capacity and removal efficiency were calculated using Equations (1) and (2), respectively, where q_e is the heavy metal ion concentration adsorbed on the adsorbent at equilibrium (mg of metal ion/g of adsorbent), C_0 and C_e are the initial and equilibrium concentration or final

concentration of metal ions in the solution (mg/L), V is the initial volume of the metal ion solution used (in L), and m is the mass of the adsorbent (in g).

$$q_e = \frac{(C_o - C_e)V}{m} \quad (1)$$

Table 5. Table showing the adsorption capacity/removal of heavy metal ions.

| Nanomaterial Used | Target Ions | Temperature | pH | Contact Time | Ion Concentration | The Capacity of Adsorption and Removal/Detection Limit | Ref. |
|--|--|--|--------------------------|--------------|--|--|-------|
| Copper doped zeolite | Cr ³⁺ Pb ²⁺ Cd ²⁺ | Room temperature for 60 min and kept in refrigerator prior to analysis | 7.5 to 2 before analysis | 60 min | 0.658 mg/L 0.696 mg/L 0.795 mg/L | 100% 100% 99.37% | [104] |
| CuO NPs | Hg ²⁺ Cr ⁶⁺ | Room temperature | 7.27 | 180 min | 1 g/L | 82% 85% | [105] |
| Cu NPs | Cr ⁶⁺ | 25 °C | 3 | 180 min | 20 mg/mL | 13.1 mg/g (65.6%) | [106] |
| CuFe ₂ O ₄ | Ba ²⁺ | 25 °C | 7 | 120 min | 10 mg in 25 mL | 87 mg/g | [107] |
| CuFe ₂ O ₄ /rGO | Ba ²⁺ | 25 °C | 7 | 120 min | 10 mg in 25 mL | 162 mg/g | [107] |
| CuFe ₂ O ₄ /PANI | UO ₂ ²⁺ (Uranium ions) | 25 °C | 4 | 60 min | | 322.6 mg/g | [76] |
| CuO NPs | Pb (II) Ni (II) Cd (II) Co (II) | Room temperature | 6 | 60 min | 0.33g/L | 88.80 mg/g 54.90 mg/g 15.60 mg/g 73.2% | [108] |
| CuO NPs | Pb (II) Ni (II) Cd (II) Cr(VI) | Sunlight | 6.6 | 200 min | 2 mg/mL | 80.8% 72.4% 64.4% 91.4% | [109] |
| Fluorescent CuO NPs | Bi ³⁺ | Room temperature | 2.7 | 15 min | 50 µL | 10 mmol L ⁻¹ | [25] |

The removal efficiency was calculated using Equation (2), and the equilibrium concentration of heavy metals (mg/L), respectively.

$$\text{Removal} = \frac{(C_o - C_e)}{C_o} \times 100 \quad (2)$$

4.3. Copper-Based Nanomaterials in Wastewater Treatment

As a result of rapid industrialization, the volume of pollutants has increased. Industrial by-products often include dangerous and cancer-causing synthetic organic dyes, pesticides, pharmaceuticals, and textile waste. If these materials are not disposed of properly, they can have a detrimental effect on the environment. Manufacturing processes often use synthetic organic dyes which are highly stable and do not break down easily. As a result, the wastewater can be toxic to humans, animals, and plants, and it can contaminate surface- and groundwater [110,111]. This can lead to serious environmental issues due to the compounds' ability to remain stable in the environment [26].

Many conventional methods such as photocatalytic degradation, coagulation, advanced oxidation processes, etc., have been used to remove pollutants from water and wastewater. These methods are less effective in meeting the stringent standards of water quality, and many emerging technologies have evolved [112]. Due to the pore size, the high surface area of the nanomaterials which has unique properties, such as photosensitivity, antimicrobial activity, catalytic activity, magnetic, electrochemical, and optical properties, provides a wide range of applications in the field of remediation of pollutants, detection, and water quality monitoring [113,114]. Many persistent pollutants, after long-term exposure, cause chronic diseases in animals and humans. For instance, 4-nitrophenol is widely used in the manufacture of drugs, dyes, insecticides and fungicides, and leather industries. Organic dyes have acute effects in humans that cause headaches, nausea, cyanosis, and irritation to the eyes [115,116]. Detection of such organic chemicals is vital in drinking and other sources of water. In a study, the copper-oxide-reduced graphene oxide nano

composite was synthesized for its enhanced catalytic activity towards the reduction of 4-nitrophenol [117].

A research study discusses the synthesis of CuS QDs@ZnO hybrid nanocomposites as an environmentally friendly preparation to improve the performance of a ZnO nanorod photocatalyst for the degradation of dyes, pharmaceuticals, and pesticides in water under simulated sunlight. The XRD, SEM, and TEM analysis results showed that the CuS QDs@ZnO hybrid nanocomposite had a high crystallinity and smaller sphere size of 2 nm. It was further found that the crystallinity and light absorption, as well as degradation activity, increased with increasing the ratio of CuS up to 3%, but then decreased with further increase. The 3% CuS QDs@ZnO hybrid nanocomposite had the capability to reduce the electron-hole recombination rate, which enhanced its degradation rate of organic pollutants [26].

4.4. Copper-Based Materials as Biosensing Materials

Graphene oxide (GO) and copper oxide (CuO) nanocomposites were used to successfully create an enzyme-free amperometric glucose biosensor using a fluorine-doped tin oxide (FTO) substrate [61]. In the presence of phosphate-buffered solution at pH 7.0, glucose sensing was performed. It was shown that the prepared sensor exhibited excellent electrical conductivity, and a low detection limit in human serum in comparison, which is perhaps due to the large superficial area that leads to good catalytic activity. The glucose sensing mechanism is given in Figure 4.

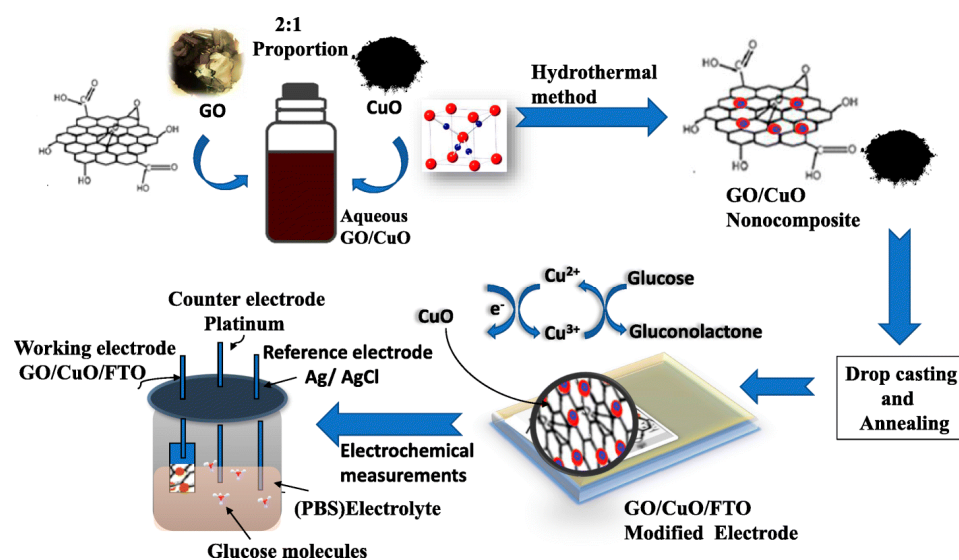


Figure 4. Biosensing mechanism of GO-CuO-FTO-modified electrode [61].

The investigation of DNA methylation, a crucial biological process, holds significance as it can alter the activity of DNA segments without modifying their sequence. Methylation of DNA has been observed to frequently impede gene transcription, especially when it takes place at a gene promoter. This understanding underscores the importance of studying DNA methylation and its impact on gene regulation. DNA methylation is crucial for proper growth in mammals and is also associated with aging, genomic imprinting, carcinogenesis, X-chromosome inactivation, and so on. In a study, modified reduced graphene oxide (rGO) which was decorated on CuNPs was used as the framework for a label-free DNA-based electrochemical biosensor that might be employed as a diagnostic tool for a DNA methylation assay [60]. Table 6 provides an outline of the recent research showing the copper nanomaterial's response towards bioanalytes.

Some small molecules, such as H_2O_2 , are key players in the design of many biosensors. H_2O_2 is a substrate in enzymatic reactions and can be used as an electron mediator or oxidizer in electrochemical reactions. It is also used to detect the activity of certain enzymes,

such as glucose oxidase, in biosensors. Additionally, H₂O₂ can be used to detect the activity of certain proteins, such as cytochrome c, in biosensors [118–120].

Table 6. Copper nanomaterial as a biosensor and its response towards bioanalytes.

| Nanomaterial | Analyte | LOD/ Detection Limit | Linear Range (mM) | Sensitivity ($\mu\text{Acm}^{-2}/\text{nM}$) /Response Time | Electrochemical Method Used | Ref. |
|--|------------------------------|----------------------------|--|---|--------------------------------|-------|
| CuO/rGO | Ascorbic acid | 189.05 μM | 500–2000 μM | - | CV | [63] |
| CuO.GdO NSs/Nafion/GCE | Glutamate | 166×10^{-6} | 166×10^{-6} to 100×10^3 | 0.567 | I-V | [51] |
| Cu-TiO ₂ | Enzyme-less myoglobin | 14 pM | 3–15 nM | 61.51 /10 ms | CV-EIS | [121] |
| Cu/Cu ₂ O | Cholesterol oxidation | 2.6 μM | 0.5 to 1 mM | 850 | CV | [20] |
| Cu ₂ O | Glucose | 1.37 μM | 0.28–2.8 mM | | LDI-MS | [17] |
| Cu/ZnO | Enzyme-less myoglobin | 0.46nM | 3 nM–15 nM | ~2.13–10.14 | CV-EIS | [122] |
| CuO- MWCNTs/SPCE | Glutamate | 17.5 μM | 20–200 μM | 8500 | LSV | [123] |
| Cu-ZnO nanorods | Hydrogen peroxide | 0.16 μM | 0.001–11 mM | 3415 | CV | [124] |
| CuO | Non-enzymatic lactic acid | 0.04 mM | 0.05–40 mM | 14.47 | CV | [125] |
| Copper phthalo cyanine-borophene nanocomposite | Non-enzymatic Urea | 0.05 μM | 250–1000 μM | 10.43 | CV | [126] |

CuO.GdO NSs/Nafion/GCE = CuO.GdO nanospikes/Nafion/GCE, CuO-MWCNTs/SPCE = CuO-multiwall carbon nanotubes/screen-printed carbon electrode. CV—Cyclic voltammetry; CV EIS—Cyclic voltammetry Electrical Impedance Spectroscopy; LDI MS—laser desorption/ionization mass spectrometry.

4.5. Copper-Based Nanomaterials in Pesticide Remediation in Soil

Despite being officially prohibited in many countries, several pesticides and insecticides are still in use today; for instance, endosulfan and carbofuran [127]. One of the most frequently used sulfur-containing organic molecules are dithiocarbamates, with major applications in the production of sugar, rubber manufacture, antioxidants, and antislime in paper making [128,129]. Between 25,000 and 35,000 metric tons are estimated to be consumed annually in this manner [130,131]. These dithiocarbamates are categorized into different classes, such as zineb, ferbam, maneb, etc., based on the carbon skeleton and properties [132]. In a report article, an advancement demonstrated for sensing dithiocarbamates (DTCs) in Ziram, Zineb, and Maneb pesticides by using cetyltrimethyl ammonium bromide (CTAB)-capped copper nanoparticles as the colorimetric probe. This economical probe is used for the detection of these pesticides in various juice samples [133]. In recent advances in agrochemical research, nanofertilizers provide nutrients to plants, and even replace many fertilizers, to improve crop yield and quality. Bollworm is a serious pest in the cultivation of cotton. In a study, engineered CuNPs had the potential of insecticidal activity in low doses (10 mg/L) to regulate the exogenous *Bacillus thuringiensis* microbial protein coded through BT toxin in plant tissue to improve resistance against bollworm [134].

4.6. Copper-Based Nanomaterials in the Degradation of Pharmaceutical Products

One of the three major sources of drugs and their metabolites entering the environment is the pharmaceutical industry, where they are released during the production of drugs. Poor waste management from industries, hospitals, and homes can also cause these substances to be discharged without being treated. Wastewater and sewage sludge from municipal wastewater treatment plants are considered a “dispersed” source, with drugs excreted by humans in homes, hospitals, and other health facilities entering these systems.

The use of effluents and biosolids for fertilizing purposes also contributes to the release of pharmaceuticals into the environment [135].

One of the most used strategies to detoxify contaminants of emerging concern (CECs) is bioremediation. Bioremediation involves the use of microorganisms to break down the CEC molecules into harmless by-products. Similarly, another approach to detoxifying CECs is nanoremediation. Nanoremediation involves the use of nanomaterials, such as nanoparticles, to absorb and trap the CEC molecules. Nanoparticles can be engineered to specifically target CEC molecules and have been used in a variety of environments, including soils, sediments, and aquatic systems. Nanoremediation has been shown to be more effective than bioremediation in some cases, as it can target specific CEC molecules more effectively by using physico-chemical treatments that include adsorption, oxidation, and filtration. Adsorption involves using particles, such as activated carbon, to adsorb the CEC molecules from an environment. Oxidation involves using chemical oxidants, such as ozone, to break down the CEC molecules into harmless by-products. Filtration involves the use of membrane filters to remove CEC molecules from an environment. Overall, the most effective and efficient way to detoxify CECs depends on the specific environment and the type of CEC molecules present. In some cases, a combination of different strategies may be needed to achieve the desired results. All strategies used to detoxify CECs must be environmentally friendly and use sustainable resources [136].

For example, reverse-micelle-synthesized Cu-TiO₂ nanomaterials as photocatalysts for levofloxacin degradation under visible light-emitting diode (LED) light. The reaction rate constant of the nanomaterials was 0.0347 min⁻¹, and the highest degradation efficiency achieved was 93.3%. The results indicate that the nanomaterials were able to adsorb, oxidize, and degrade levofloxacin under visible LED light [49].

Table 7 summarizes the performance of copper-based nanomaterials used in pharmaceutical drug degradation. The recorded concentration of the drug, catalyst loading, temperature/pH, degradation source, and degradation efficiency are all given. The results suggest that copper nanomaterials are promising for the degradation of pharmaceutical drugs.

Table 7. List of degradation results of some important pharmaceutical drugs using CuO NMs.

| Nanomaterial | Pharmaceutical Drug | Concentration of Drug (mg/L) | Catalyst Loading | Temperature/pH | Degradation Source | Degradation Efficiency | Ref |
|---|---------------------|------------------------------|------------------|----------------|--|------------------------|-------|
| CuO NPs | Thiazolyl blue | 100 | 20 mg/10 mL | 300 K/pH 8.0 | Sonication | 84.1% | [137] |
| M Mn-doped Cu ₂ O | Paracetamol | 15 | 1 g/L | 300 K/pH 7.0 | /120 min | 81.2% | [138] |
| ZnO-CuO/ clinoptilolite | Amoxicillin | 100 | 0.1 g/L | pH 9.0 | Sunlight | 92% | [139] |
| Zeolite/HDTMA- Br/CuS | Mefenamic acid | 100 | 0.1 g/L | RT/pH = 5.6 | Hg Lamp 200 min | 70% | [139] |
| | Metronidazole | 10 | 0.01 g/L | pH 7.0 | Sunlight | 100% (200 min) | [140] |
| CuO-GO-DE/H ₂ O ₂ | Ciprofloxacin | 50 | 2 g/L | 50 °C/pH 7.0 | Ultrasonic impregnation | 240 min | [62] |
| Sulfite-activated Fe-Cu | Sulfamethazine | 5 | 80 mg/L | 298 K/pH 6.0 | Advanced oxidation process | 87% (60 min) | [141] |
| Cu-TiO ₂ | Levofloxacin | 50 | 1 g/L | pH 7.0 | Visible LED | 75.5% (6 h) | [49] |
| Ba/Bi/Fe/CuO | Paracetamol | 50 | 0.75 g/L | pH 9.0 | Metal halide lamp J(HQI- T250/OSRAM GmbH) | 98.1% (120 min) | [142] |
| CuS QDs@ZnO | ceftriaxone | - | 0.2 g/L | RT | Solar simulator | 100% (90 min) | [26] |

HDTMA—Hexadecyltrimethylammonium; GO-DE—Graphene oxide diatomite.

4.7. Copper-Based Nanomaterials as VOC Sensors

VOC (Volatile Organic Compound) sensing is necessary in industries to ensure that the air quality is safe for both employees and on the roads to ensure safe driving of individuals, as alcohol intoxication is the primary cause of road accidents in the U.S. and worldwide [143]. By monitoring levels of VOCs, industries can ensure they are compliant with safety regulations and that their workers are not exposed to dangerous levels of these compounds. Prolonged exposure to VOCs can lead to respiratory problems and kidney damage; some VOCs have been linked to an increased risk of certain types of

cancers, such as leukemia and lymphoma, and long-term exposure leads to headaches, dizziness, memory loss, and other neurological effects [144]. Some molecules, such as ammonia, hydrogen sulfide, hydrogen peroxide, etc., are considered VOC biomarkers and their detection plays a vital role. For instance, ammonia in the exhaled breath indicates several diseases, such as type II Alzheimer's, kidney failure, hepatic encephalopathy, and liver dysfunction [145]. Copper has been used as a sensor for VOCs for over a decade and has proven to be a reliable and cost-effective method for detecting these compounds. Table 8 shows various techniques for deposition and applications of copper sensors to sense volatile organic compounds (VOCs).

Table 8. List of some pure and doped copper sensors for the detection of volatile organic compounds.

| Materials | Fabrication Technique/Detection System | Response time/Response (R_p/R_a) /Sensitivity (Seconds) | Linear Range | Analytes | Retention Time/Recovery Time/LOD (Seconds) | Ref |
|--|---|---|--|-------------------------------|--|-------|
| SnO ₂ -CuO | Slurry coated on ceramic tube | 4 | 50 to 300 ppm | Ethanol | 10 | [146] |
| CuO-rGO | Gas sensor | 10.54 | 100 ppm | Ethanol | 25 | [147] |
| CuO/Ti ₃ C ₂ TxMXene | Drop casting on printed IDE | 11.4 | 2.3 to 50 ppm | Toluene | 10 | [73] |
| CNNS-Cu | Deposited on glassy carbon electrode | Immediate detection | 0.1–100 $\mu\text{mol L}^{-1}$ | p-nitro toluene | 0.13 $\mu\text{mol L}^{-1}$ | [148] |
| NiO-CuO/NH ₃ sensor | Drop casting on printed IDE | 11.7 | 25 ppm to 500 ppm | NH ₃ | 21.5 | [16] |
| PEDOT-CuO | Drop casting on GCE | 2 | 40–10,000 ppm | H ₂ O ₂ | 8.5 μm | [149] |
| CeO ₂ /CuO | Deposited on Al ₂ O ₃ sensor substrate on IDE | | 90–457 ppb | Acetone | 670 | [50] |
| PNIPAM-Cu@CP | Electrodepositing Cu particles on carbon paper electrode | 72.8 $\mu\text{A cm}^{-2} \text{mM}^{-1}$ | 1–300 mM | Methanol | 0.3 mM | [150] |
| Copper nitro prusside | Deposited on the glassy carbon electrode | 15 | 2.5×10^{-8} to 2.5×10^{-1} M | Acetaldehyde | 41×10^{-8} M | [74] |
| 4HQ-rGO/Cu ²⁺ | Deposited on IDE | 5 | 1000 ppm | Acetic acid | 24 | [75] |
| AgCu/TiO ₂ | Coated on Alumina substrate for KSGAS6S KENOSISTEC | 22/33 | 100 ppm | Xylene | 33.2 | [151] |

IDE—Interdigitated electrodes; CNNS—Graphite carbon nitride nanosheets; GCE—Glassy carbon electrode; PNIPAM—Polymer N-isopropylacrylamide; 4HQ—4-Hydroxyquinoline.

4.8. Copper-Based Nanomaterials in On-Site Sensing

On-site sensing strategies for the detection of environmental contaminants play a crucial role in environmental monitoring and pollution management. These strategies enable real-time or near real-time analysis of contaminants directly at the site of interest, providing valuable information for decision-making, remediation efforts, and ensuring the safety of ecosystems and human populations. The development of on-site sensing technologies has seen significant advancements in recent years, offering increased sensitivity, selectivity, portability, and ease of use. Recent technological advances and novel scientific developments have been made in fabricating efficient point-of-care technologies, portable devices, and miniaturized tools for the on-site detection of hazardous contaminants [152–154]. These emerging technological approaches make the screening of hazardous contaminants more strategic, highly efficient, executable, rapid to operate, and cost-effective. Moreover, the design and development of on-site sensing technologies has transformed the proficiency of environmental contaminant detection. On-site sensing assays range from minimal techniques to complex and advanced investigating tools and a plethora of recognition formats. Compared to conventional and traditional sensing strategies, the use of point-of-care technologies for the on-site detection of environmental contaminants shows significant advantages with respect to the integration, levels of automation, input consumption, miniaturization, reliability, turnaround velocity, size of device, precision, ease of use, and initial detection of environmental contaminants. Furthermore, their great compatibility with different sensing strategies has prominently contributed to the cumulative demand for the point-of-care technologies. On-site sensing strategies, portable devices, and point-of-care

technologies have been integrated with laptops or smartphones or miniaturized electronic readouts for the recognition of several environmental materials.

A fluorescence-sensing strategy for sulfide (S^{2-}) detection has been developed based on the tunable interaction between MIL-53(Fe) and KA-Cu NCs (kojic acid-functional copper nanoclusters) [155]. The introduction of MIL-53(Fe) forms Fe-O bonds with KA on the surface of Cu NCs, leading to fluorescence quenching. However, the presence of S^{2-} blocks the Fe-O bond formation by occupying the Fe-site in MIL-53(Fe), resulting in a “turn-on” fluorescence signal. The constructed sensor exhibited high sensitivity with a low detection limit of 18.6 nM and a wide linear detection range from 0.05 to 5 μ M. The sensor was successfully applied to analyze water samples and food additives, demonstrating its practicality and reliability. It highlights the potential of tunable MOF-Cu NC interactions in constructing fluorescence sensing systems, opening up opportunities for various applications in the analytical field, albeit with the need to address interference from complex sample matrices.

Another study presents a one-minute synthesis of green fluorescent copper nanoclusters (TG-CuNCs) using simple sonication and 1-Thio- β -D-glucose as a capping ligand [156]. The TG-CuNCs exhibited an emission maximum at 430 nm and were characterized using various techniques. The addition of Hg^{2+} and S^{2-} ions to TG-CuNCs resulted in fluorescence quenching, enabling the detection of Hg^{2+} and S^{2-} ions with low detection limits of 1.7 nM and 1.02 nM, respectively. The synthesized TG-CuNCs were successfully applied for the detection of Hg^{2+} and S^{2-} in tap, river, and pond water. Additionally, a smartphone-aided paper-based kit was developed for on-site monitoring of Hg^{2+} and S^{2-} ions, marking the first report of such a kit using TG-CuNCs. This work highlights the potential of TG-CuNCs and the paper-based kit for applications in biosensing, material science, and nanotechnology. Like these, on-siting strategies play a vital role in environmental monitoring, pollution control, and risk assessment, enabling timely actions to protect ecosystems and human health. Continued advancements in sensing technologies and their integration with data analytics and communication platforms hold promising prospects for further improving the efficiency and effectiveness of on-site sensing systems in environmental applications.

4.9. Copper-Based Nanomaterials in Carbon Dioxide Reduction

CO_2 electroreduction can transform intermittent energy sources into high-energy chemicals, reducing dependence on fossil fuels and pollution. Products like hydrocarbons and methanol, with high energy density, are compatible with existing infrastructures and can substitute for fossil fuels [157].

CuO-ZnO nanomaterials are employed as catalysts for the conversion of carbon dioxide into methanol. Converting carbon dioxide into methanol determined that bimetallic systems combined with porous supports, such as zeolite and activated carbon, had a greater efficiency when compared to unsupported materials. Hydrogenation at different temperatures was carried out in a stainless-steel-packed bed reactor for the conversion to methanol, which indeed reduced the environmental emissions of carbon dioxide emissions [158].

In a certain CO_2 reduction experiment, which was conducted electrochemically in two compartments of H-cell in ethylene production, copper oxide nanoparticles were used as the catalyst. The ethylene production was dependent on the morphology of the catalyst. The CuO nanoparticles were deposited on conductive carbon materials which were activated, and the copper species converted to Cu^+ , which eventually resulted in the formation of 70% ethylene and 30% of hydrogen Faradaic efficiency (FE) without any other by-products in an aqueous solution [159].

The listed data reveal the surface morphology of various copper catalyst surfaces on the faradaic efficiency of carbon products that had been reported in Table 9.

Table 9. Comparison of reported FE of resultant products over copper electrocatalysts.

| Nanomaterial | Experimental Condition | Potential | Products | Faradic Efficiency | Ref. |
|---|---|-------------------|---|--------------------|-------|
| Cu _{2-x} Se _y branched CuO NPs | 41.5 mA/cm ² 0.1 M KHCO ₃ 3.0 V (vs. Ag/AgCl) | -1.815 V | Methanol | 77.6% | [157] |
| | | - | C ₂ H ₄ | 65% | [159] |
| Porous-Cu | 0.25 mg/cm ² 49 mA/cm ² | -0.976 V vs. RHE | Methane Ethylene CO | 27% 17% 10% | [160] |
| | | | | | |
| Cu-X X = Nafion, PVDF | 0.1 M KHCO ₃ -0.6 V | -1.4 V (vs. RHE) | HCOOH, CH ₄ | 30% | [161] |
| CuPc/C | 0.5 M KHCO ₃ | -0.4 V vs. RHE | Ethylene | 42.6% | [162] |
| Cu/NC | -4.9 mA/cm ² | -0.8 V vs. RHE | Formate Acetate | 40.9% 16% | [163] |
| | | | | | |
| Cu ₉₅ Sn ₅ | 0.1 M KHCO ₃ 6.58 mA/cm ² 0 V to -1.1 V vs. RHE | -0.9 V vs. RHE | CO | 93% | [164] |
| | | | | | |
| CuO | 0.1 M KHCO ₃ 50 mA/cm ² | -1.1 V | C ₂ H ₄ | 41% | [165] |
| | -2 V (vs. Ag/AgCl); -3.0 A/cm ² ; 0.5 M NaHCO ₃ | -1.0 V vs. RHE | C ₂ H ₄ , C ₂ H ₆ | - | [166] |
| Cu/Cu _x O PCC | 0.5 M KHCO ₃ -0.1 V to -1.1 V vs. RHE | -0.5 V vs. RHE | C ₂ H ₅ OH | 50% | [167] |

RHE—reversible hydrogen electrode; Por-Cu—copper (II)-5,10,15,20-tetrakis(2,6-dihydroxyphenyl) porphyrin (PorCu); CuPc/C—Copper phthalocyanine on carbon; Cu/NC—N-doped carbon-nanosheet-supported copper nanoparticles; Cu/Cu_xO PCC—Cu/Cu_xO nanoparticles embedded on porous carbon cuboids.

Figure 5 shows the CO₂ reduction of ethanol production over Cu/Cu_xO PCC electrocatalyst at low overpotential. The amount of Cu/Cu_xO nanoparticles embedded in the carbon–nitrogen network altered through varying the leaching time with nitric acid. Leaching the cuboids for 1 h (Cu/Cu_xO-PCC-1 h) led to 1.93 at% copper and leaching for 6 h (Cu/Cu_xO-PCC-6 h) ended in 0.86 at%, while the unleached cuboids showed 16.93 at% Cu content material determined from evaluating copper to carbon peaks in XPS spectra. The leaching effect was studied in terms of CO₂ reactivity and was proven to significantly increase the materials' surface area, increase the porosity, adjust the nitrogen nature, and dissipate the Cu nanoparticles. The impact of these parameters became meditated inside the materials' electrochemical performances. This shows that improving the materials' porosity and surface region cannot have a positive effect without owning a sufficient number of catalytic active sites. Similarly, pyridinic nitrogen content was shown to be correlated with improved electrocatalytic overall performance.

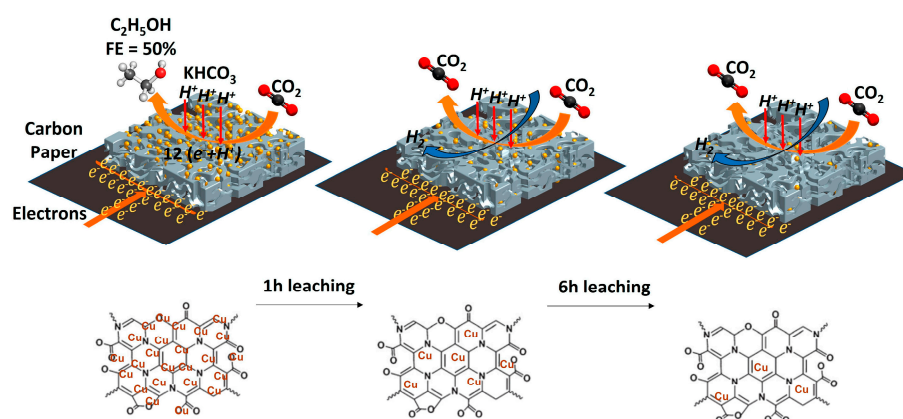


Figure 5. Cu/Cu_xO PCC catalyst for electrochemical CO₂ reduction to ethanol production [167].

5. Challenges and Perspectives

Key challenges in utilizing copper nanomaterials for pollutant degradation, wastewater treatment, and carbon dioxide reduction is optimizing their reactivity. Factors such as the size, morphology, and surface chemistry of the nanomaterials can significantly influence their catalytic activity. Finding the optimal combination of these factors to enhance reactivity and improve overall performance is a challenge that researchers need to address. Copper nanomaterials can undergo surface oxidation or agglomeration over time, leading to a decrease in their catalytic activity and stability. Ensuring the long-term stability and durability of copper nanomaterials under operating conditions, particularly in complex and harsh environments, is crucial for their practical application. Strategies such as surface modification or encapsulation can be explored to enhance their stability. Achieving high selectivity and specificity in pollutant degradation, wastewater treatment, and carbon dioxide reduction processes is a challenge. Copper nanomaterials may exhibit diverse catalytic pathways, leading to the formation of undesired by-products or incomplete pollutant removal. Developing strategies to enhance the selectivity and specificity of copper nanomaterials towards target pollutants is an important area of research. Scaling up the production of copper nanomaterials and integrating them into practical systems for large-scale pollutant degradation, wastewater treatment, or carbon dioxide reduction applications is a challenge. Ensuring cost-effectiveness and feasibility in terms of material synthesis, fabrication techniques, and system integration is essential for their practical implementation. The cost of copper nanomaterials can be a significant challenge for their widespread application in pollutant degradation, wastewater treatment, and carbon dioxide reduction. Strategies to reduce production costs, such as optimizing synthesis methods, exploring alternative raw materials, or developing scalable fabrication techniques, need to be investigated. Cost-effective production processes will enhance the feasibility and practicality of utilizing copper nanomaterials in environmental applications. Ensuring the reusability of copper nanomaterials is crucial for sustainable and cost-effective environmental remediation. However, the fouling or deactivation of catalyst surfaces over time can reduce their effectiveness and require frequent replacement. Developing strategies to regenerate or reactivate copper nanomaterials, such as surface cleaning techniques or catalyst rejuvenation methods, is essential for their long-term viability and economic viability.

Future research can focus on tailoring the design and engineering of copper nanomaterials for specific pollutant degradation, wastewater treatment, and carbon dioxide reduction applications. This includes optimizing the composition, size, shape, and surface properties of copper nanomaterials to enhance their catalytic activity, selectivity, and stability. Exploring synergistic approaches by combining copper nanomaterials with other catalysts or materials can enhance their performance. Hybrid catalyst systems, such as bimetallic or composite nanomaterials, can provide synergistic effects that improve catalytic activity, selectivity, and durability. Advancements in characterization techniques, such as in

situ spectroscopy, microscopy, and surface science methods, can provide insights into the reaction mechanisms and surface properties of copper nanomaterials. This knowledge can guide the rational design of improved catalysts with enhanced performance. Integrating copper-nanomaterial-based catalytic systems with renewable energy sources, such as solar or wind energy, can enable sustainable pollutant degradation, wastewater treatment, and carbon dioxide reduction processes. Exploring the synergies between copper nanomaterials and renewable energy technologies can contribute to the development of more sustainable and efficient systems. While pollutant degradation, wastewater treatment, and carbon dioxide reduction are key areas of focus, there are additional environmental applications where copper nanomaterials can be explored. This includes applications such as sensors for pollutant detection, antimicrobial coatings, or remediation of specific environmental contaminants. Developing methods for the recycling and recovery of copper nanomaterials from spent catalysts or wastewater treatment systems. Effective recovery techniques will not only reduce the environmental impact associated with the disposal of used nanomaterials but also provide a cost-effective approach by reusing valuable copper resources. Exploring the integration of copper nanomaterials with support materials or matrices can enhance their reusability. Hybrid catalyst systems, where copper nanomaterials are anchored or encapsulated within a stable support, can provide mechanical protection and prevent leaching, thereby extending their lifespan and facilitating their reusability. Investigating regeneration strategies for copper nanomaterials can contribute to their reusability. This may involve developing techniques to remove fouling species or reactivating the catalytic surfaces through controlled surface modifications or surface cleaning processes. Regeneration approaches can enhance the longevity and performance of copper nanomaterials, reducing the need for frequent replacement. Conducting comprehensive life-cycle assessments and economic evaluations of copper-nanomaterial-based systems can provide insights into their cost-effectiveness and environmental impact. Assessing the entire life cycle, from synthesis to disposal or recycling, will help identify opportunities for improvement and optimize the overall economic and environmental sustainability of copper nanomaterial applications. Integrating copper nanomaterials into a circular economy framework can enhance their reusability and minimize waste. This involves designing systems where the by-products or outputs of one process become the inputs for another, ensuring a closed-loop approach and reducing the reliance on unexplored materials.

6. Conclusions

In conclusion, copper-based nanomaterials have shown great promise for environmental remediation such as wastewater treatment (dyes, pesticides, and heavy metal removal), biosensing, VOC sensors, and CO₂ reduction, etc. This extensive article summarizes many efficient methods proposed mainly to examine and assess recent publications on Cu-based materials and give an overall view and identify potential future work areas in the remediation of the environment. Even though many promising biological methods are found to be safer, Cu NPs are biocompatible and non-toxic, and are capable of removing hazardous metals from contaminated water, soil, and air, as well as breaking down toxic organic compounds, making them ideal for use in environmental remediation. However, for perfect environmental management, research should not be confined to detection, but potential future work and further investigations should be extended in different areas of synergetic effects in environmental management in the areas of reduction, degradation, reuse, recycling, etc. With further research, copper-based nanomaterials could be used to effectively clean up many types of contaminated environments, ultimately leading to a healthier and safer world for everyone. By providing an extensive overview of recent advancements and highlighting the unique contributions of copper-based nanomaterials, this review serves as a valuable resource for researchers. The novelty lies in its emphasis on sustainable approaches to environmental remediation and its potential applications, including pollutant degradation, wastewater treatment, and carbon dioxide reduction. Addressing challenges related to reactivity optimization, stability, selectivity, scalability,

cost-effectiveness, and reusability will pave the way for future advancements in utilizing copper nanomaterials for sustainable environmental applications (pollutant degradation, wastewater treatment, and carbon dioxide reduction) applications. Opportunities lie in catalyst design, synergistic approaches, advanced characterization techniques, integration with renewable energy sources, and exploring new environmental applications beyond degradation. Exploring recycling and recovery strategies, hybrid systems, regeneration techniques, and conducting comprehensive life-cycle analyses will contribute to the practical implementation and economic viability of copper nanomaterials for environmental remediation applications. Embracing circular economy approaches will further enhance the sustainability and reusability of copper nanomaterials, promoting their long-term use in environmental remediation efforts. Future studies can benefit from the insights presented here to advance the utilization of copper nanomaterials, enabling effective and sustainable solutions for environmental remediation.

Author Contributions: Writing—original draft preparation, S.B., S.R.B. and R.P.; writing—review, editing, and supervision, R.B.; visualization, R.K.S. and A.B.R.; project administration and funding acquisition, N.A.-Q. All authors have read and agreed to the published version of the manuscript.

Funding: This work was supported by Qatar University through a National Capacity Building Program Grant (NCBP), [QUCP-CAM-20/23-463]. Statements made herein are solely the responsibility of the authors.

Institutional Review Board Statement: Not applicable.

Data Availability Statement: Data are contained within the article.

Conflicts of Interest: The authors declare no conflict of interest.

Abbreviations

| | |
|---------------------|--|
| AFM | Atomic force microscopy |
| BET | Brunauer–Emmett–Teller |
| CNTs | Carbon nanotubes |
| CuO | Copper oxide (CuO) |
| CVD | Chemical vapor deposition |
| DCS | Differential centrifugal sedimentation |
| DLS | Dynamic light scattering |
| DRS | Diffuse-reflectance spectroscopy |
| EPM | Electrophoretic mobility |
| FESEM | Field emission scanning electron microscopy |
| FT-IR | Fourier transform infrared. |
| FTO | Fluorine-doped tin oxide |
| GO | Graphene oxide |
| HRTEM | High-Resolution Transmission Electron Microscopy |
| LSPR | Localized surface plasmon resonance |
| MA-SiO ₂ | Methacrylate-functionalized silica |
| MOFs | Metal organic frameworks |
| MRI | Magnetic resonance imaging |
| NPs | Nanoparticles |
| PEC | Photoelectrochemical |
| PEG | Polyethylene glycol |
| PEO | Polyethylene oxide (PEO) |
| PL | Photoluminescence |
| PLA | Polylactic acid |
| PNP | Polymer nanoparticle |
| PVD | Physical vapor deposition |
| RET | Resonant energy transfer |
| SERS | Surface-enhanced Raman spectroscopy |
| SQUID | Superconducting quantum interference device magnetometry |

| | |
|---------|--|
| TEM | Transmittance electron microscopy |
| TMD-NDs | Transition-metal dichalcogenide nanodots |
| UV-Vis | UV-Vis Spectroscopy |
| VSM | Vibrating sample magnetometry |
| XPS | X-ray photon spectroscopy |
| XRD | X-ray diffraction |

References

1. Yang, C.; Bromma, K.; Sung, W.; Schuemann, J.; Chithrani, D. Determining the Radiation Enhancement Effects of Gold Nanoparticles in Cells in a Combined Treatment with Cisplatin and Radiation at Therapeutic Megavoltage Energies. *Cancers* **2018**, *10*, 150. [[CrossRef](#)] [[PubMed](#)]
2. Fratoddi, I.; Cartoni, A.; Venditti, I.; Catone, D.; O’Keeffe, P.; Paladini, A.; Toschi, F.; Turchini, S.; Sciubba, F.; Testa, G.; et al. Gold nanoparticles functionalized by rhodamine B isothiocyanate: A new tool to control plasmonic effects. *J. Colloid Interface Sci.* **2018**, *513*, 10–19. [[CrossRef](#)] [[PubMed](#)]
3. Neuschmelting, V.; Harmsen, S.; Beziere, N.; Lockau, H.; Hsu, H.-T.; Huang, R.; Razansky, D.; Ntziachristos, V.; Kircher, M.F. Dual-Modality Surface-Enhanced Resonance Raman Scattering and Multispectral Optoacoustic Tomography Nanoparticle Approach for Brain Tumor Delineation. *Small* **2018**, *14*, 1800740. [[CrossRef](#)]
4. Zaera, F. Nanostructured materials for applications in heterogeneous catalysis. *Chem. Soc. Rev.* **2013**, *42*, 2746–2762. [[CrossRef](#)] [[PubMed](#)]
5. Mwanza, N.D.; Shigwenya, M.E.; Makhanu, S.D.; Victor, O.B.; Gachoki, K.P.; Kinoti, K.P. Environmental remediation using nanomaterial as adsorbents for emerging micropollutants. *Environ. Nanotechnol. Monit. Manag.* **2023**, *20*, 100789. [[CrossRef](#)]
6. Khalaj, M.; Kamali, M.; Khodaparast, Z.; Jahanshahi, A. Copper-based nanomaterials for environmental decontamination—An overview on technical and toxicological aspects. *Ecotoxicol. Environ. Saf.* **2018**, *148*, 813–824. [[CrossRef](#)]
7. Crisan, M.C.; Teodora, M.; Lucian, M. Copper Nanoparticles: Synthesis and Characterization, Physiology, Toxicity and Antimicrobial Applications. *Appl. Sci.* **2022**, *12*, 141. [[CrossRef](#)]
8. Sandoval, S.S.; Silva, N. Review on Generation and Characterization of Copper Particles and Copper Composites Prepared by Mechanical Milling on a Lab-Scale. *Int. J. Mol. Sci.* **2023**, *24*, 7933. [[CrossRef](#)]
9. Hong, X.; Zhu, H.; Du, D.; Zhang, Q.; Li, Y. Research Progress of Copper-Based Bimetallic Electrocatalytic Reduction of CO₂. *Catalysts* **2023**, *13*, 376. [[CrossRef](#)]
10. Naz, S.; Gul, A.; Zia, M.; Javed, R. Synthesis, biomedical applications, and toxicity of CuO nanoparticles. *Appl. Microbiol. Biotechnol.* **2023**, *107*, 1039–1061. [[CrossRef](#)]
11. Rubilar, O.; Rai, M.; Tortella, G.; Diez, M.C.; Seabra, A.B.; Durán, N. Biogenic nanoparticles: Copper, copper oxides, copper sulphides, complex copper nanostructures and their applications. *Biotechnol. Lett.* **2013**, *35*, 1365–1375. [[CrossRef](#)] [[PubMed](#)]
12. Biswas, A.; Bayer, I.S.; Biris, A.S.; Wang, T.; Dervishi, E.; Faupel, F. Advances in top-down and bottom-up surface nanofabrication: Techniques, applications & future prospects. *Adv. Colloid Interface Sci.* **2012**, *170*, 2–27. [[CrossRef](#)] [[PubMed](#)]
13. Lu, W.; Lieber, C.M. Nanoelectronics from the bottom up. *Nat. Mater.* **2007**, *6*, 841–850. [[CrossRef](#)] [[PubMed](#)]
14. Mijatovic, D.; Eijkel, J.C.T.; van Den Berg, A. Technologies for nanofluidic systems: Top-down vs. bottom-up—A review. *Lab A Chip* **2005**, *5*, 492–500. [[CrossRef](#)] [[PubMed](#)]
15. Pothu, R.; Challa, P.; Rajesh, R.; Boddula, R.; Balaga, R.; Balla, P.; Perugopu, V.; Radwan, A.B.; Abdullah, A.M.; Al-Qahtani, N. Vapour-Phase Selective Hydrogenation of γ -Valerolactone to 2-Methyltetrahydrofuran Biofuel over Silica-Supported Copper Catalysts. *Nanomaterials* **2022**, *12*, 3414. [[CrossRef](#)]
16. Rumana, H.; Kamrul, H.; Veena, S. Utilising problematic waste to detect toxic gas release in the environment: Fabricating a NiO doped CuO nanoflake based ammonia sensor from e-waste. *Nanoscale Adv.* **2022**, *4*, 4066–4079. [[CrossRef](#)]
17. Li, K.; Xu, X.; Liu, W.; Yang, S.; Huang, L.; Tang, S.; Zhang, Z.; Wang, Y.; Chen, F.; Qian, K. A Copper-Based Biosensor for Dual-Mode Glucose Detection. *Front. Chem.* **2022**, *10*, 861353. [[CrossRef](#)]
18. Liu, Q.M.; Yasunami, T.; Kuruda, K.; Okido, M. Preparation of Cu nanoparticles with ascorbic acid by aqueous solution reduction method. *Trans. Nonferrous Met. Soc. China* **2012**, *22*, 2198–2203. [[CrossRef](#)]
19. Mott, D.; Galkowski, J.; Wang, L.; Luo, J.; Zhong, C.J. Synthesis of Size-Controlled and Shaped Copper Nanoparticles. *Langmuir* **2007**, *23*, 5740–5745. [[CrossRef](#)]
20. Espinosa-Lagunes, F.I.; Cruz, J.C.; Vega-Azamar, R.E.; Murillo-Borbonio, I.; Torres-González, J.; Escalona-Villalpando, R.A.; Gurrola, M.P.; Ledesma-García, J.; Arriaga, L.G. Copper nanoparticles suitable for bifunctional cholesterol oxidation reaction: Harvesting energy and sensor. *Mater. Renew. Sustain. Energy* **2022**, *11*, 105–114. [[CrossRef](#)]
21. Rao, M.P.C.; Kulandaivelu, K.; Ponnusamy, V.K.; Wu, J.J.; Sambandam, A. Surfactant-assisted synthesis of copper oxide nanorods for the enhanced photocatalytic degradation of Reactive Black 5 dye in wastewater. *Environ. Sci. Pollut. Res.* **2019**, *27*, 17438–17445. [[CrossRef](#)]
22. Lu, R.; Hao, W.; Kong, L.; Zhao, K.; Bai, H.; Liu, Z. A simple method for the synthesis of copper nanoparticles from metastable intermediates. *RSC Adv.* **2023**, *13*, 14361–14369. [[CrossRef](#)] [[PubMed](#)]
23. Lastovina, T.A.; Budnyk, A.P.; Khaishbashev, G.A.; Egor, A. Kudryavtsev, E.A.; Soldatov, A.V. Copper-based nanoparticles prepared from copper(II) acetate bipyridine complex. *J. Serb. Chem. Soc.* **2016**, *81*, 751–762. [[CrossRef](#)]

24. Ahamed, M.; Lateef, R.; Akhtar, M.J.; Rajanahalli, P. Dietary Antioxidant Curcumin Mitigates CuO Nanoparticle-Induced Cytotoxicity through the Oxidative Stress Pathway in Human Placental Cells. *Molecules* **2022**, *27*, 7378. [[CrossRef](#)]
25. Wu, R.; Ai, J.; Ga, L. Synthesis of Fluorescent Copper Nanomaterials and Detection of Bi³⁺. *Front. Chem.* **2022**, *10*, 899672. [[CrossRef](#)] [[PubMed](#)]
26. Mohammed, R.; Ali, M.E.M.; Gomaa, E.; Mohsen, M. Copper sulfide and zinc oxide hybrid nanocomposite for wastewater decontamination of pharmaceuticals and pesticides. *Sci. Rep.* **2022**, *12*, 18153. [[CrossRef](#)]
27. Jardón-Maximino, N.; Pérez-Alvarez, M.; Cadenas-Pliego, G.; Lugo-Urbe, L.E.; Cabello-Alvarado, C.; Mata-Padilla, J.M.; Barriga-Castro, E.D. Synthesis of Copper Nanoparticles Stabilized with Organic Ligands and Their Antimicrobial Properties. *Polymers* **2021**, *13*, 2846. [[CrossRef](#)]
28. Khlifi, N.; Mnif, S.; Ben Nasr, F.; Fourati, N.; Zerrouki, C.; Chehimi, M.M.; Guerhazi, H.; Aifa, S. Non-doped and transition metal-doped CuO nano-powders: Structure-physical properties and anti-adhesion activity relationship. *RSC Adv.* **2022**, *12*, 23527–23543. [[CrossRef](#)]
29. Badawy, S.M.; El Khashab, R.; Nayl, A. Synthesis, Characterization and Catalytic Activity of Cu/Cu₂O Nanoparticles Prepared in Aqueous Medium. *Bull. Chem. React. Eng. Catal.* **2015**, *10*, 169–174. [[CrossRef](#)]
30. Guzman, M.; Arcos, M.; Dille, J.; Godet, S.; Rousse, C. Effect of the Concentration of NaBH₄ and N₂H₄ as Reductant Agent on the Synthesis of Copper Oxide Nanoparticles and its Potential Antimicrobial Applications. *Nano Biomed. Eng.* **2018**, *10*, 392–405. [[CrossRef](#)]
31. Guzman, M.; Arcos, M.; Dille, J.; Rousse, C.; Godet, S.; Malet, L. Effect of the Concentration and the Type of Dispersant on the Synthesis of Copper Oxide Nanoparticles and Their Potential Antimicrobial Applications. *ACS Omega* **2021**, *6*, 18576–18590. [[CrossRef](#)]
32. Guzman, M.; Tian, W.; Walker, C.; Herrera, J.E. Copper oxide nanoparticles doped with lanthanum, magnesium and manganese: Optical and structural characterization. *R. Soc. Open Sci.* **2022**, *9*, 220485. [[CrossRef](#)] [[PubMed](#)]
33. Ponnar, M.; Thangamani, C.; Monisha, P.; Gomathi, S.; Pushpanathan, K. Influence of Ce doping on CuO nanoparticles synthesized by microwave irradiation method. *Appl. Surf. Sci.* **2018**, *449*, 132–143. [[CrossRef](#)]
34. Mersian, H.; Alizadeh, M.; Hadi, N. Synthesis of zirconium doped copper oxide (CuO) nanoparticles by the Pechini route and investigation of their structural and antibacterial properties. *Ceram. Int.* **2018**, *44*, 20399–20408. [[CrossRef](#)]
35. Ganesan, K.P.; Anandhan, N.; Gopu, G.; Amaliroselin, A.; Marimuthu, T.; Paneerselvam, R. An enhancement of ferromagnetic, structural, morphological, and optical properties of Mn-doped Cu₂O thin films by an electrodeposition technique. *J. Mater. Sci.* **2019**, *30*, 19524–19535. [[CrossRef](#)]
36. Rapp, R.A.; Ezis, A.; Yurek, G.J. Displacement reactions in the solid state. *Met. Trans.* **1973**, *4*, 1283–1292. [[CrossRef](#)]
37. Luo, F.; Wei, J.; Liu, Q.; Wang, J. The study of room temperature ferromagnetism in Mn-doped Cu₂O powders. *Mater. Sci. Semicond. Process.* **2021**, *133*, 105972. [[CrossRef](#)]
38. Sathiyavimal, S.; Vasantharaj, S.; Bharathi, D.; Saravanan, M.; Manikandan, E.; Kumar, S.S.; Pugazhendhi, A. Biogenesis of copper oxide nanoparticles (CuONPs) using *Sida acuta* and their incorporation over cotton fabrics to prevent the pathogenicity of Gram negative and Gram positive bacteria. *J. Photochem. Photobiol. B Biol.* **2018**, *188*, 126–134. [[CrossRef](#)]
39. Ahmad, H.; Venugopal, K.; Bhat, A.H.; Kavitha, K.; Ramanan, A.; Rajagopal, K.; Srinivasan, R.; Manikandan, E. Enhanced Biosynthesis Synthesis of Copper Oxide Nanoparticles (CuO-NPs) for their Antifungal Activity Toxicity against Major Phyto-Pathogens of Apple Orchards. *Pharm. Res.* **2020**, *37*, 246. [[CrossRef](#)] [[PubMed](#)]
40. Kardarian, K.; Nunes, D.; Sberna, P.M.; Ginsburg, A.; Keller, D.A.; Pinto, J.V.; Deuermeier, J.; Anderson, A.Y.; Zaban, A.; Martins, R.; et al. Effect of Mg doping on Cu₂O thin films and their behavior on the TiO₂/Cu₂O heterojunction solar cells. *Sol. Energy Mater. Sol. Cells* **2016**, *147*, 27–36. [[CrossRef](#)]
41. Resende, J.; Jiménez, C.; Nguyen, N.D.; Deschanvres, J.-L. Magnesium-doped cuprous oxide (Mg:Cu₂O) thin films as a transparent p-type semiconductor. *Phys. Status Solidi (A)* **2016**, *213*, 2296–2302. [[CrossRef](#)]
42. Ivill, M.; Overberg, M.; Abernathy, C.; Norton, D.; Hebard, A.; Theodoropoulou, N.; Budai, J. Properties of Mn-doped Cu₂O semiconducting thin films grown by pulsed-laser deposition. *Solid-State Electron.* **2003**, *47*, 2215–2220. [[CrossRef](#)]
43. Das, K.; Sharma, S.N.; Kumar, M.; De, S.K. Luminescence properties of the solvothermally synthesized blue light emitting Mn doped Cu₂O nanoparticles. *J. Appl. Phys.* **2010**, *107*, 024316. [[CrossRef](#)]
44. Suganthi, A.; Vethanathan, S.J.K.; Perumal, S.; Koilpillai, D.P.; Karpagavalli, S. Optical and Electrical Properties of Solvothermally Synthesized Manganese Doped Cuprous Oxide Nanoparticles. *IOSR J. Appl. Phys.* **2017**, *1*, 43–48. [[CrossRef](#)]
45. Jacob, S.S.K.; Kulandaisamy, I.; Valanarasu, S.; Arulanantham, A.M.S.; Ganesh, V.; AlFaify, S.; Kathalingam, A. Enhanced optoelectronic properties of Mg doped Cu₂O thin films prepared by nebulizer pyrolysis technique. *J. Mater. Sci. Mater. Electron.* **2019**, *30*, 10532–10542. [[CrossRef](#)]
46. Zhao, Z.-B.; Liu, J.-D.; Du, X.-Y.; Wang, Z.-Y.; Zhang, C.; Ming, S.-F. Fabrication of silver nanoparticles/copper nanoparticles jointly decorated nitride flakes to improve the thermal conductivity of polymer composites. *Colloids Surf. A Physicochem. Eng. Asp.* **2022**, *635*, 128104. [[CrossRef](#)]
47. Hanh, T.T.; Chi, N.T.L.; Duy, N.N. Preparation of Copper Nanoparticles/Diatomite Nanocomposite for Improvement in Water Quality of Fishponds. *J. Chem.* **2022**, *2022*, 3921631. [[CrossRef](#)]
48. Habte, A.G.; Hone, F.G.; Dejene, F.B. Influence of Cu-Doping Concentration on the Structural and Optical Properties of SnO₂ Nanoparticles by Coprecipitation Route. *J. Nanomater.* **2022**, *2022*, 5957125. [[CrossRef](#)]

49. Varma, K.S.; Shukla, A.D.; Tayade, R.J.; Joshi, P.A.; Das, A.K.; Modi, K.B.; Gandhi, V.G. Photocatalytic performance and interaction mechanism of reverse micelle synthesized Cu-TiO₂ nanomaterials towards levofloxacin under visible LED light. *Photochem. Photobiol. Sci.* **2022**, *21*, 77–89. [[CrossRef](#)] [[PubMed](#)]
50. Oosthuizen, D.N.; Weber, I.C. A Strategy to Enhance Humidity Robustness of p-Type CuO Sensors for Breath Acetone Quantification. *Small Sci.* **2023**, *3*, 2200096. [[CrossRef](#)]
51. Rahman, M.M.; Hussain, M.M.; Asiri, A.M.; Alamry, K.; Hasnat, M. An enzyme free detection of L-Glutamic acid using deposited CuO.GdO nanospikes on a flat glassy carbon electrode. *Surf. Interfaces* **2020**, *20*, 100617. [[CrossRef](#)]
52. Abebe, B.; Tsegaye, D.; Sori, C.; Prasad, R.C.K.R.; Murthy, H.C.A. Cu/CuO-Doped ZnO Nanocomposites via Solution Combustion Synthesis for Catalytic 4-Nitrophenol Reduction. *ACS Omega* **2023**, *8*, 9597–9606. [[CrossRef](#)]
53. Ye, L.; He, X.; Obeng, E.; Wang, D.; Zheng, D.; Shen, T.; Shen, J.; Hu, R.; Deng, H. The CuO and AgO co-modified ZnO nano-composites for promoting wound healing in Staphylococcus aureus infection. *Mater. Today Bio* **2023**, *18*, 100552. [[CrossRef](#)] [[PubMed](#)]
54. Chandrasekar, M.; Subash, M.; Logambal, S.; Udhayakumar, G.; Uthrakumar, R.; Inmozhi, C.; Al-Onazi, W.A.; Al-Mohaimed, A.M.; Chen, T.-W.; Kanimozhi, K. Synthesis and characterization studies of pure and Ni doped CuO nanoparticles by hydrothermal method. *J. King Saud Univ. Sci.* **2022**, *34*, 101831. [[CrossRef](#)]
55. El-Hout, S.; El-Sheikh, S.; Hassan, H.M.; Harraz, F.A.; Ibrahim, I.; El-Sharkawy, E. A green chemical route for synthesis of graphene supported palladium nanoparticles: A highly active and recyclable catalyst for reduction of nitrobenzene. *Appl. Catal. A Gen.* **2015**, *503*, 176–185. [[CrossRef](#)]
56. Cheng, Y.; Fan, Y.; Pei, Y.; Qiao, M. Graphene-supported metal/metal oxide nanohybrids: Synthesis and applications in heterogeneous catalysis. *Catal. Sci. Technol.* **2015**, *5*, 3903–3916. [[CrossRef](#)]
57. Ma, B.; Wang, Y.; Tong, X.; Guo, X.; Zheng, Z.; Guo, X. Graphene-supported CoS₂ particles: An efficient photocatalyst for selective hydrogenation of nitroaromatics in visible light. *Catal. Sci. Technol.* **2017**, *7*, 2805–2812. [[CrossRef](#)]
58. Goswami, A.; Rath, A.K.; Aparicio, C.; Tomanec, O.; Petr, M.; Pocklanova, R.; Gawande, M.B.; Varma, R.S.; Zboril, R. In Situ Generation of Pd–Pt Core–Shell Nanoparticles on Reduced Graphene Oxide (Pd@Pt/rGO) Using Microwaves: Applications in Dehalogenation Reactions and Reduction of Olefins. *ACS Appl. Mater. Interfaces* **2017**, *9*, 2815–2824. [[CrossRef](#)]
59. Zhang, K.; Suh, J.M.; Lee, T.H.; Cha, J.H.; Choi, J.-W.; Jang, H.W.; Varma, R.S.; Shokouhimehr, M. Copper oxide–graphene oxide nanocomposite: Efficient catalyst for hydrogenation of nitroaromatics in water. *Nano Converg.* **2019**, *6*, 6. [[CrossRef](#)]
60. Sedlackova, E.; Bytesnikova, Z.; Birgusova, E.; Svec, P.; Ashrafi, A.M.; Estrela, P.; Richtera, L. Label-Free DNA Biosensor Using Modified Reduced Graphene Oxide Platform as a DNA Methylation Assay. *Materials* **2020**, *13*, 4936. [[CrossRef](#)]
61. Gijare, M.; Chaudhari, S.; Ekar, S.; Garje, A. A facile synthesis of GO/CuO-blended nanofiber sensor electrode for efficient enzyme-free amperometric determination of glucose. *J. Anal. Sci. Technol.* **2021**, *12*, 40. [[CrossRef](#)]
62. Zhang, T.; Zhang, J.; Yu, Y.; Li, J.; Zhou, Z.; Li, C. Synthesis of CuO/GO-DE Catalyst and Its Catalytic Properties and Mechanism on Ciprofloxacin Degradation. *Nanomaterials* **2022**, *12*, 4305. [[CrossRef](#)]
63. Singh, A.; Sharma, A.; Ahmed, A.; Arya, S. Highly selective and efficient electrochemical sensing of ascorbic acid via CuO/rGO nanocomposites deposited on conductive fabric. *Appl. Phys. A* **2022**, *128*, 262. [[CrossRef](#)]
64. Katowah, D.F.; Saleh, S.M.; Alqarni, S.A.; Ali, R.; Mohammed, G.I.; Hussein, M.A. Network structure-based decorated CPA@CuO hybrid nanocomposite for methyl orange environmental remediation. *Sci. Rep.* **2021**, *11*, 5056. [[CrossRef](#)] [[PubMed](#)]
65. Malik, M.A.; Surepally, R.; Akula, N.; Cheedarala, R.K.; Alshehri, A.A.; Alzahrani, K.A. Oxidation of Alcohols into Carbonyl Compounds Using a CuO@GO Nano Catalyst in Oxygen Atmospheres. *Catalysts* **2023**, *13*, 55. [[CrossRef](#)]
66. Hajjipour, P.; Bahrami, A.; Eslami, A.; Hosseini-Abari, A.; Hagh Ranjbar, H.R. Chemical bath synthesis of CuO-GO-Ag nanocomposites with enhanced antibacterial properties. *J. Alloys Compd.* **2020**, *821*, 153456. [[CrossRef](#)]
67. Janmee, N.; Preechakasedkit, P.; Rodthongkum, N.; Chailapakul, O.; Potiyaraj, P.; Ruecha, N. A non-enzymatic disposable electrochemical sensor based on surface-modified screen-printed electrode CuO-IL/rGO nanocomposite for a single-step determination of glucose in human urine and electrolyte drinks. *Anal. Methods* **2021**, *13*, 2796–2803. [[CrossRef](#)] [[PubMed](#)]
68. Zhang, Z.; Sun, L.; Wu, Z.; Liu, Y.; Li, S. Facile hydrothermal synthesis of CuO–Cu₂O/GO nanocomposites for the photocatalytic degradation of organic dye and tetracycline pollutants. *New J. Chem.* **2020**, *44*, 6420–6427. [[CrossRef](#)]
69. Bekru, A.G.; Tufa, L.T.; Zelekew, O.A.; Gwak, J.; Lee, J.; Sabir, F.K. Microwave-Assisted Synthesis of rGO-ZnO/CuO Nanocomposites for Photocatalytic Degradation of Organic Pollutants. *Crystals* **2023**, *13*, 133. [[CrossRef](#)]
70. Krishna, R.; Fernandes, D.M.; Ventura, J.; Freire, C.; Titus, E. Novel synthesis of highly catalytic active Cu@Ni/RGO nanocomposite for efficient hydrogenation of 4-nitrophenol organic pollutant. *Int. J. Hydrog. Energy* **2016**, *41*, 11608–11615. [[CrossRef](#)]
71. Pérez-Poyatos, L.; Pastrana-Martínez, L.; Morales-Torres, S.; Sánchez-Moreno, P.; Bramini, M.; Maldonado-Hódar, F. Iron-copper oxide nanoparticles supported on reduced graphene oxide for the degradation of cyclophosphamide by photo-Fenton reaction. *Catal. Today* **2023**, 114010, (under press). [[CrossRef](#)]
72. Shah, A.H.; Abideen, Z.U.; Maqsood, S.; Rashid, F.; Ullah, R.; Rehman, A.U.; Dildar, M.; Ahmad, M.; Ullah, K.; Rafi, M.N.; et al. Porous Cu-based metal organic framework (Cu-MOF) for highly selective adsorption of organic pollutants. *J. Solid State Chem.* **2023**, *322*, 123935. [[CrossRef](#)]
73. Hermawan, A.; Zhang, B.; Taufik, A.; Asakura, Y.; Hasegawa, T.; Zhu, J.; Shi, P.; Yin, S. CuO Nanoparticles/Ti₃C₂T_x MXene Hybrid Nanocomposites for Detection of Toluene Gas. *ACS Appl. Nano Mater.* **2020**, *3*, 4755–4766. [[CrossRef](#)]

74. Esokkiya, A.; Murugasenapathi, N.; Kumar, S.; Sudalaimani, S.; Santhosh, B.; Tamilarasan, P.; Sivakumar, C.; Giribabu, K. Electrochemically activated copper nitroprusside as a catalyst for sensing of carcinogenic acetaldehyde in red wine. *Sens. Actuators B Chem.* **2022**, *363*, 131798. [[CrossRef](#)]
75. Gong, Y.; Li, H.; Pei, W.; Fan, J.; Umar, A.; Al-Assiri, M.S.; Wang, Y.; de Rooij, N.F.; Zhou, G. Assembly with copper(ii) ions and D- π -A molecules on a graphene surface for ultra-fast acetic acid sensing at room temperature. *RSC Adv.* **2019**, *9*, 30432–30438. [[CrossRef](#)]
76. Feng, X.; Sun, S.; Cheng, G.; Shi, L.; Yang, X.; Zhang, Y. Removal of Uranyl Ion from Wastewater by Magnetic Adsorption Material of Polyaniline Combined with CuFe₂O₄. *Adsorpt. Sci. Technol.* **2021**, *2021*, 5584158. [[CrossRef](#)]
77. Fan, W.; Wang, A.; Wang, L.; Jiang, X.; Xue, Z.; Li, J.; Wang, G. Hollow Carbon Nanopillar Arrays Encapsulated with Pd–Cu Alloy Nanoparticles for the Oxygen Evolution Reaction. *ACS Appl. Mater. Interfaces* **2023**, *15*, 13600–13608. [[CrossRef](#)]
78. Mourdikoudis, S.; Pallares, R.M.; Thanh, N.T.K. Characterization techniques for nanoparticles: Comparison and complementarity upon studying nanoparticle properties. *Nanoscale* **2018**, *10*, 12871–12934. [[CrossRef](#)]
79. Wang, Y.; Sun, H.; Ang, H.M.; Tadó, M.O.; Wang, S. 3D-hierarchically structured MnO₂ for catalytic oxidation of phenol solutions by activation of peroxymonosulfate: Structure dependence and mechanism. *Appl. Catal. B Environ.* **2015**, *164*, 159–167. [[CrossRef](#)]
80. Wang, L.; Ke, F.; Zhu, J. Metal–organic gel templated synthesis of magnetic porous carbon for highly efficient removal of organic dyes. *Dalton Trans.* **2016**, *45*, 4541–4547. [[CrossRef](#)]
81. Dong, F.; Guo, W.; Park, S.-S.; Ha, C.-S. Uniform and monodisperse polysilsesquioxane hollow spheres: Synthesis from aqueous solution and use in pollutant removal. *J. Mater. Chem.* **2011**, *21*, 10744–10749. [[CrossRef](#)]
82. Khan, I.; Saeed, K.; Zekker, I.; Zhang, B.; Hendi, A.H.; Ahmad, A.; Ahmad, S.; Zada, N.; Ahmad, H.; Shah, L.A.; et al. Review on Methylene Blue: Its Properties, Uses, Toxicity and Photodegradation. *Water* **2022**, *14*, 242. [[CrossRef](#)]
83. Khan, S.A.; Khan, S.B.; Asiri, A.M. Toward the design of Zn–Al and Zn–Cr LDH wrapped in activated carbon for the solar assisted de-coloration of organic dyes. *RSC Adv.* **2016**, *6*, 83196–83208. [[CrossRef](#)]
84. Khan, S.A.; Khan, S.B.; Asiri, A.M. Layered double hydroxide of Cd–Al/C for the Mineralization and De-coloration of Dyes in Solar and Visible Light Exposure. *Sci. Rep.* **2016**, *6*, 35107. [[CrossRef](#)]
85. Wang, C.; Salmon, L.; Li, Q.; Igartua, M.E.; Moya, S.; Ciganda, R.; Ruiz, J.; Astruc, D. From Mono to Tris-1,2,3-triazole-Stabilized Gold Nanoparticles and Their Compared Catalytic Efficiency in 4-Nitrophenol Reduction. *Inorg. Chem.* **2016**, *55*, 6776–6780. [[CrossRef](#)] [[PubMed](#)]
86. Mandal, S.; De, S. Catalytic and fluorescence studies with copper nanoparticles synthesized in polysorbates of varying hydrophobicity. *Colloids Surf. A Physicochem. Eng. Asp.* **2015**, *467*, 233–250. [[CrossRef](#)]
87. Pakzad, K.; Alinezhad, H.; Nasrollahzadeh, M. Green synthesis of Ni@Fe₃O₄ and CuO nanoparticles using Euphorbia maculata extract as photocatalysts for the degradation of organic pollutants under UV-irradiation. *Ceram. Int.* **2019**, *45*, 17173–17182. [[CrossRef](#)]
88. Bordbar, M.; Sharifi-Zarchi, Z.; Khodadadi, B. Green synthesis of copper oxide nanoparticles/clinoptilolite using Rheum palmatum L. root extract: High catalytic activity for reduction of 4-nitro phenol, rhodamine B, and methylene blue. *J. Sol-Gel Sci. Technol.* **2016**, *81*, 724–733. [[CrossRef](#)]
89. Alshaikhi, H.A.; Asiri, A.M.; Alamry, K.A.; Marwani, H.M.; Alfifi, S.Y.; Khan, S.B. Copper Nanoparticles Decorated Alginate/Cobalt-Doped Cerium Oxide Composite Beads for Catalytic Reduction and Photodegradation of Organic Dyes. *Polymers* **2022**, *14*, 4458. [[CrossRef](#)]
90. Cosma, D.; Urda, A.; Radu, T.; Rosu, M.C.; Mihet, M.; Socaci, C. Evaluation of the Photocatalytic Properties of Copper Oxides/Graphene/TiO₂ Nanoparticles Composites. *Molecules* **2022**, *27*, 5803. [[CrossRef](#)]
91. Ahsan, H.; Shahid, M.; Imran, M.; Mahmood, F.; Siddique, M.H.; Ali, H.M.; Niazi, M.B.; Hussain, S.; Shahbaz, M.; Ayyub, M.; et al. Photocatalysis and adsorption kinetics of azo dyes by nanoparticles of nickel oxide and copper oxide and their nanocomposite in an aqueous medium. *PeerJ* **2022**, *10*, e14358. [[CrossRef](#)]
92. Chandan, M.R.; Kumar, K.R.; Shaik, A.H. Two-dimensional Cu nanostructures for efficient photo-catalytic degradation of methylene blue. *Environ. Sci. Adv.* **2022**, *1*, 814–826. [[CrossRef](#)]
93. Borge, V.V.; Patil, R.M.; Dwivedi, P.R. Photocatalytic Decomposition of Rhodamine B Dye Using Copper Oxide Nanoparticles Prepared from Copper Chalcone Complexes. *Int. J. Nanosci.* **2022**, *21*, 2250039. [[CrossRef](#)]
94. Nazim, M.; Khan, A.A.P.; Asiri, A.M.; Kim, J.H. Exploring Rapid Photocatalytic Degradation of Organic Pollutants with Porous CuO Nanosheets: Synthesis, Dye Removal, and Kinetic Studies at Room Temperature. *ACS Omega* **2021**, *6*, 2601–2612. [[CrossRef](#)]
95. Ajibade, P.A.; Oluwalana, A.E. Enhanced Photocatalytic Degradation of Ternary Dyes by Copper Sulfide Nanoparticles. *Nanomaterials* **2021**, *11*, 2000. [[CrossRef](#)]
96. Rasheed, S.; Batool, Z.; Intisar, A.; Riaz, S.; Shaheen, M.; Kousar, R. Enhanced photodegradation activity of cuprous oxide nanoparticles towards Congo red for water purification. *Desalination Water Treat.* **2021**, *227*, 330–337. [[CrossRef](#)]
97. Nahar, B.; Chaity, S.B.; Gafur, A.; Hossain, M.Z. Synthesis of Spherical Copper Oxide Nanoparticles by Chemical Precipitation Method and Investigation of Their Photocatalytic and Antibacterial Activities. *J. Nanomater.* **2023**, *2023*, 2892081. [[CrossRef](#)]
98. Aksu, Z. Application of biosorption for the removal of organic pollutants: A review. *Process. Biochem.* **2005**, *40*, 997–1026. [[CrossRef](#)]
99. Ahluwalia, S.S.; Goyal, D. Microbial and plant derived biomass for removal of heavy metals from wastewater. *Bioresour. Technol.* **2007**, *98*, 2243–2257. [[CrossRef](#)]

100. Mukherjee, A.G.; Renu, K.; Gopalakrishnan, A.V.; Veeraraghavan, V.P.; Vinayagam, S.; Paz-Montelongo, S.; Dey, A.; Vellingiri, B.; George, A.; Madhyastha, H.; et al. Heavy Metal and Metalloid Contamination in Food and Emerging Technologies for Its Detection. *Sustainability* **2023**, *15*, 1195. [[CrossRef](#)]
101. Madadrang, C.J.; Kim, H.Y.; Gao, G.; Wang, N.; Zhu, J.; Feng, H.; Gorrington, M.; Kasner, M.L.; Hou, S. Adsorption Behavior of EDTA-Graphene Oxide for Pb (II) Removal. *ACS Appl. Mater. Interfaces* **2012**, *4*, 1186–1193. [[CrossRef](#)]
102. Witkowska, D.; Slowik, J.; Chilicka, K. Heavy Metals and Human Health: Possible Exposure Pathways and the Competition for Protein Binding Sites. *Molecules* **2021**, *26*, 6060. [[CrossRef](#)] [[PubMed](#)]
103. Haso, H.W.; Dubale, A.A.; Chimdesa, M.A.; Atlabachew, M. High Performance Copper Based Metal Organic Framework for Removal of Heavy Metals From Wastewater. *Front. Mater.* **2022**, *9*, 840806. [[CrossRef](#)]
104. Fanta, F.T.; Dubale, A.A.; Bebizuh, D.F.; Atlabachew, M. Copper doped zeolite composite for antimicrobial activity and heavy metal removal from waste water. *BMC Chem.* **2019**, *13*, 44. [[CrossRef](#)]
105. Raul, P.K.; Das, B.; Umlong, I.M.; Devi, R.R.; Tiwari, G.; Kamboj, D.V. Toward a Feasible Solution for Removing Toxic Mercury and Chromium From Water Using Copper Oxide Nanoparticles. *Front. Nanotechnol.* **2022**, *4*, 805698. [[CrossRef](#)]
106. Sikder, T.; Mihara, Y.; Islam, S.; Saito, T.; Tanaka, S.; Kurasaki, M. Preparation and characterization of chitosan–cooxymethyl- β -cyclodextrin entrapped nanozero-valent iron composite for Cu (II) and Cr (IV) removal from wastewater. *Chem. Eng. J.* **2014**, *236*, 378–387. [[CrossRef](#)]
107. Mary, B.C.J.; Vijaya, J.J.; Bououdina, M.; Khezami, L.; Modwi, A.; Ismail, M.; Bellucci, S. Study of Barium Adsorption from Aqueous Solutions Using Copper Ferrite and Copper Ferrite/rGO Magnetic Adsorbents. *Adsorpt. Sci. Technol.* **2022**, *2022*, 3954536. [[CrossRef](#)]
108. Mahmoud, A.E.D.; Al-Qahtani, K.M.; Alflaj, S.O.; Al-Qahtani, S.F.; Alsamhan, F.A. Green copper oxide nanoparticles for lead, nickel, and cadmium removal from contaminated water. *Sci. Rep.* **2021**, *11*, 12547. [[CrossRef](#)]
109. Eid, A.M.; Fouda, A.; Hassan, S.E.-D.; Hamza, M.F.; Alharbi, N.K.; Elkelish, A.; Alharthi, A.; Salem, W.M. Plant-Based Copper Oxide Nanoparticles; Biosynthesis, Characterization, Antibacterial Activity, Tanning Wastewater Treatment, and Heavy Metals Sorption. *Catalysts* **2023**, *13*, 348. [[CrossRef](#)]
110. Maavia, A.; Aslam, I.; Tanveer, M.; Rizwan, M.; Iqbal, M.W.; Tahir, M.; Hussain, H.; Boddula, R.; Yousuf, M. Facile synthesis of g-C₃N₄/CdWO₄ with excellent photocatalytic performance for the degradation of Minocycline. *Mater. Sci. Energy Technol.* **2019**, *2*, 258–266. [[CrossRef](#)]
111. Sriram, G.; Bendre, A.; Mariappan, E.; Altalhi, T.; Kigga, M.; Ching, Y.C.; Jung, H.-Y.; Bhaduri, B.; Kurkuri, M. Recent trends in the application of metal-organic frameworks (MOFs) for the removal of toxic dyes and their removal mechanism—A review. *Sustain. Mater. Technol.* **2022**, *31*, e00378. [[CrossRef](#)]
112. Ighalo, J.O.; Sagboye, P.A.; Umenweke, G.; Ajala, O.J.; Omoarukhe, F.O.; Adeyanju, C.A.; Ogunniyi, S.; Adeniyi, A.G. CuO nanoparticles (CuO NPs) for water treatment: A review of recent advances. *Environ. Nanotechnol. Monit. Manag.* **2021**, *15*, 100443. [[CrossRef](#)]
113. Sharma, N.; Singh, G.; Sharma, M.; Mandzhieva, S.; Minkina, T.; Rajput, V.D. Sustainable Use of Nano-Assisted Remediation for Mitigation of Heavy Metals and Mine Spills. *Water* **2022**, *14*, 3972. [[CrossRef](#)]
114. Qu, X.; Alvarez, P.J.; Li, Q. Applications of nanotechnology in water and wastewater treatment. *Water Res.* **2014**, *47*, 3931–3946. [[CrossRef](#)] [[PubMed](#)]
115. Haleem, A.; Shafiq, A.; Chen, S.-Q.; Nazar, M. A Comprehensive Review on Adsorption, Photocatalytic and Chemical Degradation of Dyes and Nitro-Compounds over Different Kinds of Porous and Composite Materials. *Molecules* **2023**, *28*, 1081. [[CrossRef](#)] [[PubMed](#)]
116. Shanmugam, P.; Ngullie, R.C.; Smith, S.M.; Boonyuen, S.; Boddula, R.; Pothu, R. Visible-light induced photocatalytic removal of methylene blue dye by copper oxide decorated zinc oxide nanorods. *Mater. Sci. Energy Technol.* **2023**, *6*, 359–367. [[CrossRef](#)]
117. Sarkar, C.; Dolui, S.K. Synthesis of copper oxide/reduced graphene oxide nanocomposite and its enhanced catalytic activity towards reduction of 4-nitrophenol. *RSC Adv.* **2015**, *75*, 60763–60769. [[CrossRef](#)]
118. Patel, V.; Kruse, P.; Selvaganapathy, P.R. Solid State Sensors for Hydrogen Peroxide Detection. *Biosensors* **2021**, *11*, 9. [[CrossRef](#)]
119. Miao, Z.; Zhang, D.; Chen, Q. Non-enzymatic Hydrogen Peroxide Sensors Based on Multi-wall Carbon Nanotube/Pt Nanoparticle Nanohybrids. *Materials* **2014**, *7*, 2945–2955. [[CrossRef](#)]
120. Meier, J.; Hofferber, E.M.; Stapleton, J.A.; Iverson, N.M. Hydrogen Peroxide Sensors for Biomedical Applications. *Chemosensors* **2019**, *7*, 64. [[CrossRef](#)]
121. Umar, A.; Haque, M.; Ansari, S.G.; Seo, H.-K.; Ibrahim, A.A.; Alhamami, M.A.M.; Algadi, H.; Ansari, Z.A. Label-Free Myoglobin Biosensor Based on Pure and Copper-Doped Titanium Dioxide Nanomaterials. *Biosensors* **2022**, *12*, 1151. [[CrossRef](#)]
122. Haque, M.; Fouad, H.; Seo, H.-K.; Alothman, O.Y.; Ansari, Z.A. Cu-Doped ZnO Nanoparticles as an Electrochemical Sensing Electrode for Cardiac Biomarker Myoglobin Detection. *IEEE Sens. J.* **2020**, *20*, 8820–8832. [[CrossRef](#)]
123. Ali, Y.; Knight, D.; Howlader, M.M.R. Nonenzymatic Electrochemical Glutamate Sensor Using Copper Oxide Nanomaterials and Multiwall Carbon Nanotubes. *Biosensors* **2023**, *13*, 237. [[CrossRef](#)] [[PubMed](#)]
124. Arsalan, M.; Saddique, I.; Baoji, M.; Awais, A.; Khan, I.; Shamseldin, M.A.; Mehrez, S. Novel Synthesis of Sensitive Cu-ZnO Nanorod-Based Sensor for Hydrogen Peroxide Sensing. *Front. Chem.* **2022**, *10*, 932985. [[CrossRef](#)]
125. Sajna, M.; Cabibihan, J.-J.; Malik, R.A.; Sadasivuni, K.K.; Geetha, M.; Alahmad, J.K.; Hijazi, D.A.; Alsaedi, F. Nonenzymatic electrochemical lactic acid sensor using CuO nanocomposite. *Mater. Sci. Eng. B* **2023**, *288*, 116217. [[CrossRef](#)]

126. Güngör, S.; Taşaltın, C.; Gürol, I.; Baytemir, G.; Karakuş, S.; Taşaltın, N. Copper phthalocyanine-borophene nanocomposite-based non-enzymatic electrochemical urea biosensor. *Appl. Phys. A* **2022**, *128*, 89. [[CrossRef](#)]
127. Saputra, F.; Uapipatanakul, B.; Lee, J.-S.; Hung, S.-M.; Huang, J.-C.; Pang, Y.-C.; Muñoz, J.E.R.; Macabeo, A.P.G.; Chen, K.H.-C.; Hsiao, C.-D. Co-Treatment of Copper Oxide Nanoparticle and Carbofuran Enhances Cardiotoxicity in Zebrafish Embryos. *Int. J. Mol. Sci.* **2021**, *22*, 8259. [[CrossRef](#)]
128. Odularu, A.T.; Ajibade, P.A. Dithiocarbamates: Challenges, Control, and Approaches to Excellent Yield, Characterization, and Their Biological Applications. *Bioinorg. Chem. Appl.* **2019**, *2019*, 8260496. [[CrossRef](#)]
129. Malik, A.K.; Faubel, W. Methods of analysis of dithiocarbamate pesticides: A review. *Pestic. Sci.* **1999**, *55*, 965–970. [[CrossRef](#)]
130. AL ALAM, J.; Bom, L.; Chbani, A.; Fajloun, Z.; Millet, M. Analysis of Dithiocarbamate Fungicides in Vegetable Matrices Using HPLC-UV Followed by Atomic Absorption Spectrometry. *J. Chromatogr. Sci.* **2017**, *55*, 429–435. [[CrossRef](#)]
131. Ajiboye, T.O.; Ajiboye, T.T.; Marzouki, R.; Onwudiwe, D.C. The Versatility in the Applications of Dithiocarbamates. *Int. J. Mol. Sci.* **2022**, *23*, 1317. [[CrossRef](#)]
132. Szolar, O. Environmental and pharmaceutical analysis of dithiocarbamates. *Anal. Chim. Acta* **2007**, *582*, 191–200. [[CrossRef](#)] [[PubMed](#)]
133. Ghoto, S.A.; Kuhuwar, M.Y.; Jahangir, T.M.; Mangi, J.U.D. Applications of copper nanoparticles for colorimetric detection of dithiocarbamate pesticides. *J. Nanostructure Chem.* **2019**, *9*, 77–93. [[CrossRef](#)]
134. Mittal, D.; Kaur, G.; Singh, P.; Yadav, K.; Ali, S.A. Nanoparticle-Based Sustainable Agriculture and Food Science: Recent Advances and Future Outlook. *Front. Nanotechnol. Sec. Nanotechnol. Energy Appl.* **2020**, *2*, 579954. [[CrossRef](#)]
135. Gworek, B.; Kijeńska, M.; Wrzosek, J.; Graniewska, M. Pharmaceuticals in the Soil and Plant Environment: A Review. *Water Air Soil Pollut.* **2021**, *232*, 145. [[CrossRef](#)]
136. Menacherry, S.P.M.; Aravind, U.K.; Aravind Kumar, C.T. Oxidative Degradation of Pharmaceutical Waste, Theophylline, from Natural Environment. *Atmosphere* **2022**, *13*, 835. [[CrossRef](#)]
137. Akpomie, K.G.; Conradie, J. Efficient adsorptive removal of paracetamol and thiazolyl blue from polluted water onto biosynthesized copper oxide nanoparticles. *Sci. Rep.* **2023**, *13*, 859. [[CrossRef](#)]
138. Gaim, Y.T.; Yimanuh, S.M.; Kidanu, Z.G. Enhanced Photocatalytic Degradation of Amoxicillin with Mn-Doped Cu₂O under Sunlight Irradiation. *J. Compos. Sci.* **2022**, *6*, 317. [[CrossRef](#)]
139. Shirzadi, A.; Nezamzadeh-Ejehieh, A. Enhanced photocatalytic activity of supported CuO–ZnO semiconductors towards the photodegradation of mefenamic acid aqueous solution as a semi real sample. *J. Mol. Catal. A Chem.* **2016**, *411*, 222–229. [[CrossRef](#)]
140. Al-Musawi, T.J.; Moghaddam, N.S.M.; Rahimi, S.M.; Amarzadeh, M.; Nasseh, N. Efficient photocatalytic degradation of metronidazole in wastewater under simulated sunlight using surfactant- and CuS-activated zeolite nanoparticles. *J. Environ. Manag.* **2022**, *319*, 115697. [[CrossRef](#)]
141. Dong, Q.; Dong, H.; Li, Y.; Xiao, J.; Xiang, S.; Hou, X.; Chu, D. Degradation of sulfamethazine in water by sulfite activated with zero-valent Fe-Cu bimetallic nanoparticles. *J. Hazard. Mater.* **2022**, *431*, 128601. [[CrossRef](#)]
142. Abbas, H.A.; Nasr, R.A.; Vannier, R.-N.; Jamil, T.S. Improving of photocatalytic activity of barium ferrate via bismuth and copper co-doping for degradation of paracetamol under visible light irradiation. *J. Environ. Sci.* **2022**, *112*, 331–342. [[CrossRef](#)] [[PubMed](#)]
143. Benhaddouch, T.E.; Pinzon, S.K.; Landi, D.M.C.; Marcial, J.; Mehta, P.; Romero, K.; Rockward, T.; Bhansali, S.; Dong, D. Review—Micro-Fuel Cell Principal Biosensors for Monitoring Transdermal Volatile Organic Compounds in Humans. *ECS Sens. Plus* **2022**, *1*, 041602. [[CrossRef](#)]
144. Shuai, J.; Kim, S.; Ryu, H.; Park, J.; Lee, C.K.; Kim, G.-B.; Ultra, V.U., Jr.; Yang, W. Health risk assessment of volatile organic compounds exposure near Daegu dyeing industrial complex in South Korea. *BMC Public Health* **2018**, *18*, 528. [[CrossRef](#)]
145. Dima, A.C.; Balaban, D.V.; Dima, A. Diagnostic Application of Volatile Organic Compounds as Potential Biomarkers for Detecting Digestive Neoplasia: A Systematic Review. *Diagnostics* **2021**, *11*, 2317. [[CrossRef](#)] [[PubMed](#)]
146. Zhang, J.; Ma, S.; Wang, B.; Pei, S. Hydrothermal synthesis of SnO₂-CuO composite nanoparticles as a fast-response ethanol gas sensor. *J. Alloy. Compd.* **2021**, *886*, 161299. [[CrossRef](#)]
147. Meng, F.; Yang, Z.; Yuan, Z.; Zhang, H.; Zhu, H. Hydrothermal synthesis of CuO/rGO nanosheets for enhanced gas sensing properties of ethanol. *Ceram. Int.* **2023**, *49*, 5595–5603. [[CrossRef](#)]
148. Chen, L.; Li, Z.; Xiao, Q.; Li, M.; Xu, Y.; Qiu, X. Sensitive detection of p-nitrotoluene based on a copper cluster modified carbon nitride nanosheets photoelectrochemical sensor. *Appl. Catal. A Gen.* **2023**, *649*, 118964. [[CrossRef](#)]
149. Lete, C.; Spinciu, A.-M.; Alexandru, M.-G.; Moreno, J.C.; Leau, S.-A.; Marin, M.; Visinescu, D. Copper(II) Oxide Nanoparticles Embedded within a PEDOT Matrix for Hydrogen Peroxide Electrochemical Sensing. *Sensors* **2022**, *22*, 8252. [[CrossRef](#)]
150. Ma, P.; Ma, X. High-sensitivity and temperature-controlled switching methanol sensor prepared based on the dual catalysis of copper particles. *Talanta* **2022**, *237*, 122888. [[CrossRef](#)]
151. Maake, P.J.; Mokoena, T.P.; Bolokang, A.S.; Hintsho-Mbita, N.; Tshilongo, J.; Cummings, F.R.; Swart, H.C.; Iwuoha, E.I.; Motaung, D.E. Fabrication of AgCu/TiO₂ nanoparticle-based sensors for selective detection of xylene vapor. *Mater. Adv.* **2022**, *3*, 7302–7318. [[CrossRef](#)]
152. Umaphathi, R.; Park, B.; Sonwal, S.; Rani, G.M.; Cho, Y.; Huh, Y.S. Advances in optical-sensing strategies for the on-site detection of pesticides in agricultural foods. *Trends Food Sci. Technol.* **2022**, *119*, 69–89. [[CrossRef](#)]
153. Raju, C.V.; Cho, C.H.; Rani, G.M.; Manju, V.; Umaphathi, R.; Huh, Y.S.; Park, J.P. Emerging insights into the use of carbon-based nanomaterials for the electrochemical detection of heavy metal ions. *Coord. Chem. Rev.* **2023**, *476*, 214920. [[CrossRef](#)]

154. Umapathi, R.; Raju, C.V.; Ghoreishian, S.M.; Rani, G.M.; Kumar, K.; Oh, M.-H.; Park, J.P.; Huh, Y.S. Recent advances in the use of graphitic carbon nitride-based composites for the electrochemical detection of hazardous contaminants. *Coord. Chem. Rev.* **2022**, *470*, 214708. [[CrossRef](#)]
155. Hu, X.; Tang, J.; Shen, Y. Turn-on fluorescence determination of sulfide based on site-occupying modulation of MOF-copper nanocluster interaction. *Microchim. Acta* **2022**, *189*, 306. [[CrossRef](#)]
156. Maruthupandi, M.; Thirupathi, D.; Vasimalai, N. One minute synthesis of green fluorescent copper nanocluster: The preparation of smartphone aided paper-based kit for on-site monitoring of nanomolar level mercury and sulfide ions in environmental samples. *J. Hazard. Mater.* **2020**, *392*, 122294. [[CrossRef](#)]
157. Yang, D.; Zhu, Q.; Chen, C.; Liu, H.; Liu, Z.; Zhao, Z.; Zhang, X.; Liu, S.; Han, B. Selective electroreduction of carbon dioxide to methanol on copper selenide nanocatalysts. *Nat. Commun.* **2019**, *10*, 677. [[CrossRef](#)]
158. Pothu, R.; Mitta, H.; Banerjee, P.; Boddula, R.; Srivastava, R.K.; Kalambate, P.K.; Naik, R.; Radwan, A.B.; Al-Qahtani, N. Insights into the influence of Pd loading on CeO₂ catalysts for CO₂ hydrogenation to methanol. *Mater. Sci. Energy Technol.* **2023**, *6*, 484–492. [[CrossRef](#)]
159. Kim, J.; Choi, W.; Park, J.W.; Kim, C.; Kim, M.; Song, H. Branched Copper Oxide Nanoparticles Induce Highly Selective Ethylene Production by Electrochemical Carbon Dioxide Reduction. *J. Am. Chem. Soc.* **2019**, *141*, 6986–6994. [[CrossRef](#)]
160. Weng, Z.; Jiang, J.; Wu, Y.; Wu, Z.; Guo, X.; Materna, K.L.; Liu, W.; Batista, V.S.; Brudvig, G.W.; Wang, H. Electrochemical CO₂ Reduction to Hydrocarbons on a Heterogeneous Molecular Cu Catalyst in Aqueous Solution. *J. Am. Chem. Soc.* **2016**, *138*, 8076–8079. [[CrossRef](#)]
161. Chang, Q.; Lee, J.H.; Liu, Y.; Xie, Z.; Hwang, S.; Marinkovic, N.S.; Park, A.-H.A.; Kattel, S.; Chen, J.G. Electrochemical CO₂ Reduction Reaction over Cu Nanoparticles with Tunable Activity and Selectivity Mediated by Functional Groups in Polymeric Binder. *JACS Au* **2022**, *2*, 214–222. [[CrossRef](#)]
162. Li, M.; Li, T.; Wang, R.; Sun, C.; Zhang, N.; Gao, R.; Song, Y. Heat-treated copper phthalocyanine on carbon toward electrochemical CO₂ conversion into ethylene boosted by oxygen reduction. *Chem. Commun.* **2022**, *87*, 12192–12195. [[CrossRef](#)]
163. Suliman, M.H.; Yamani, Z.H.; Usman, M. Electrochemical Reduction of CO₂ to C₁ and C₂ Liquid Products on Copper-Decorated Nitrogen-Doped Carbon Nanosheets. *Nanomaterials* **2023**, *13*, 47. [[CrossRef](#)] [[PubMed](#)]
164. Pan, Y.; Wu, M.; Ye, Z.; Tang, H.; Hong, Z.; Zhi, M. Cu-Sn Aerogels for Electrochemical CO₂ Reduction with High CO selectivity. *Molecules* **2023**, *28*, 1033. [[CrossRef](#)] [[PubMed](#)]
165. Pang, Y.; Burdyny, T.; Dinh, C.-T.; Kibria, M.G.; Fan, J.Z.; Liu, M.; Sargent, E.H.; Sinton, D. Joint tuning of nanostructured Cu-oxide morphology and local electrolyte programs high-rate CO₂ reduction to C₂H₄. *Green Chem.* **2017**, *19*, 4023–4030. [[CrossRef](#)]
166. Dutta, A.; Rahaman, M.; Mohos, M.; Zanetti, A.; Broekmann, P. Electrochemical CO₂ Conversion Using Skeleton (Sponge) Type of Cu Catalysts. *ACS Catal.* **2017**, *7*, 5431–5437. [[CrossRef](#)]
167. Alkoshab, M.Q.; Thomou, E.; Abdulazeez, I.; Suliman, M.H.; Spyrou, K.; Iali, W.; Alhooshani, K.; Baroud, T.N. Low Overpotential Electrochemical Reduction of CO₂ to Ethanol Enabled by Cu/Cu_xO Nanoparticles Embedded in Nitrogen-Doped Carbon Cuboids. *Nanomaterials* **2023**, *13*, 230. [[CrossRef](#)]

Disclaimer/Publisher's Note: The statements, opinions and data contained in all publications are solely those of the individual author(s) and contributor(s) and not of MDPI and/or the editor(s). MDPI and/or the editor(s) disclaim responsibility for any injury to people or property resulting from any ideas, methods, instructions or products referred to in the content.